Chirality Transfer from Atropisomeric Chiral Inducers to Nematic and Smectic Liquid Crystals - Synthesis and Characterization of *Di*- and *Tetra*-Substituted Axially Chiral Binaphthyl Derivatives

Munju Goh †, Jinwoo Park, Yehdong Han, Sangbum Ahn, and Kazuo Akagi*

Department of Polymer Chemistry, Kyoto University, Katsura, Kyoto 615-8510, Japan

CORRESPONDING AUTHOR FOOTNOTE:

* Corresponding author E-mail: akagi@fps.polym.kyoto-u.ac.jp

† Present address: Institute of Advanced Composite Materials, Korea Institute of Science and Technology

Abstract

The chirality transfer of axially chiral binaphthyl derivatives bearing liquid crystal (LC) moieties at the *n*,*n*' positions (*n* = 3, 4, 6) of the binaphthyl rings to nematic (N) and smectic (S) LCs is investigated. Chiral nematic LCs (N*-LCs) are prepared by adding a small amount of the chiral binaphthyl derivative into host N-LCs composed of cyanobiphenyl mesogen cores. The binaphthyl derivative with phenylcyclohexyl (PCH) type LC moieties at the 4,4' positions of the binaphthyl ring [**D-4,4'**] exhibits a low helical twisting power (HTP) of 11 μm^{-1}. In contrast, those with LC moieties at the 3,3' and 6,6' positions of the binaphthyl rings [**D-3,3'** and **D-6,6'**] exhibit high HTPs of 153 μm^{-1} and 154 μm^{-1}, respectively. Next, the binaphthyl derivatives are added into two types of S-LCs with phenylbenzoate mesogen cores: 4-(4-methylpentyloxy)phenyl-4-(decyloxy)benzoate [**PhB1**] and 4-(3-methylpentyloxy)phenyl-4-(decyloxy)benzoate [**PhB2**]. The mixture of the host LC, **PhB1** or **PhB2** with the chiral dopant, **D-3,3'** or **D-6,6'** show chiral smectic LCs C (S_C*-LCs). The highly twisted S_C* phases with helical pitches of 1.2 ~ 1.4 μm are prepared in **PhB1** and **PhB2** by using the chiral dopant of **D-6,6'**. It is concluded that **D-6,6'** has a large helical twisting power and is the most favourable atropisomeric chiral inducer for chirality transfer to both N-LCs and S-LCs.

KEYWORDS: chiral dopant, binaphthyl derivative, atropisomer, chirality transfer, chiral nematic liquid crystal, chiral smectic C phase

Introduction

Chirality is a very intriguing issue in liquid crystal (LC) science.[1] There are many types of chiral LCs, such as chiral nematic (N*),[2] chiral smectic C (S_C*),[3] blue phase,[4] and twisted grain boundary (TGB) phase LCs.[5] Chiral inductions in nematic (N) and smectic C (S_C) LCs through chirality transcription by the chiral dopants have been extensively investigated.[6-11] The chiral nematic liquid crystal (N*-LC) is prepared by adding a small amount of a chiral compound as a chiral dopant (a chiral inducer) to N-LC. Additionally, the helical pitch of the N*-LC can be controlled by changing the concentration of the chiral dopant, modifying the helical twisting power (HTP) of the chiral dopant[12], and even using chirality-switchable chiral dopants that are responsive to external stimuli, such as thermal heating[13] and light irradiation.[14] N*-LCs have recently been identified as useful as asymmetric reaction fields for the synthesis of one-handed helical conjugated polymers.[12a,15] Because the helical sense and pitch of the polymers strongly depend on those of the N*-LC, understanding the potential abilities of the chiral dopants is essential. There are two main types of chiral dopants: asymmetric centre and axially chiral compounds. The latter is more promising than the former because of its large HTP and ready chemical modification, allowing the HTP to be tuned. In fact, chiral binaphthyl derivatives bearing *di*- or *tetra*-substituents at various positions of the binaphthyl rings are preferably used as chiral dopants. However, how the substituents at the binaphthyl rings affect the chirality transfer of the chiral compound to the host LCs remains unclear.

Some S_C*-LCs have been used as ferroelectric materials that quickly respond to an electric field owing to their substantially large spontaneous polarisation. Although it is possible to induce a S_C* phase by adding a chiral dopant into a S_C-LC, the formation of the S_C* phase is not always guaranteed.[16] The difficulty of chirality transfer and/or chirality induction of the chiral dopant to the host S_C-LC is due in part to (i) the chiral dopant's low miscibility in the S_C-LCs and (ii) rigidity from the highly ordered structure of the S_C-LC. The former issue (low miscibility) can be overcome by introducing LC groups as substituents into the chiral dopant, which should enhance the miscibility between the chiral dopant and the S_C-LC. The latter (rigidity) can be resolved by choosing chiral compounds with large HTPs, such as axially chiral binaphthyl derivatives.

However, one issue remains to be settled. In the S_C* phase, the director (*n*) is tilted with respect to the layer normal and precesses simultaneously about the layer normal. At the present time, it is still unclear how the tilt angle (θ), defined between the director (*n*) and the layer normal, and the precessing motion about the layer normal together produce the helical structure of the S_C* phase, although the spontaneous polarisation has been elucidated to be proportional to the sine of the tilt angle.

The axially chiral binaphthyl derivatives are typical atropisomers that are conformers arising from restricted rotation about a single bond and can be regarded as chirality sources for asymmetric catalysts, chiral recognition, and chiral oligomers and polymers.[17] The HTPs of the binaphthyl derivatives come from dual steric repulsions between substituents at the 2,2' positions and those between hydrogen atoms at the 8,8' positions of the naphthyl rings.[2] Moreover, the substituents can be inserted at various positions of the binaphthyl rings. In fact, many binaphthyl derivatives with different substituents at the 2,2'[12,13c,18]; 2,2',6,6'[12,19]; or 2,2',5,5',6,6' positions[20] have been synthesised. However, few studies comprehensively address the relationship between the substitution positions of the binaphthyl ring and the effectiveness of the chirality transcription to N- and S_C-LCs.

In this study, we have synthesised a series of axially chiral binaphthyl derivatives bearing phenylcyclohexyl (PCH) type LC groups at the *n,n*' positions (*n* = 3, 4 and 6) of the binaphthyl rings and investigated their chirality transcription abilities as chiral dopants to induce N*- and S_C*-LCs. The binaphthyl derivative of **D-6,6'**, having a direct linkage between the mesogenic core of the LC substituents and the binaphthyl rings at the 6 and 6' positions, exhibits a large HTP of 154 μm^{-1} in N-LC and is capable of inducing the S_C* phase with a helical pitch of 1.7 μm.

2. Methods

All experiments were performed under argon atmosphere. Tetrahydrofuran (THF) and dichloromethane (CH_2Cl_2) were distilled prior to use. Williamson etherification and Suzuki coupling reactions were used to obtain the chiral dopants. The chemical compounds (*R*)-2,2'-

dihydroxy-1,1'-binaphthyl (optical purity, 0.99) and 3,3'-dibromo-2,2'-dimethoxy-1,1'-binaphthyl were purchased from commercially available sources. The mesogenic compound 4-(*trans*-4-*n*-pentylcyclohexyl)bromobenzene [PCH5Br] was commercially available. Di-substituted binaphthyl derivative [(*R*)-2,2'-ethoxy-binaphthyl, abbreviated as **D-1**] was synthesised according to the literature.[12] Proton (^{1}H) nuclear magnetic resonance (NMR) spectra were measured in $CDCl_3$ using a JEOL 400 MHz NMR spectrometer. Chemical shifts are represented in parts per million downfield from tetramethylsilane as an internal standard. The chemical properties of the synthesised compounds are given in the final section. High-resolution mass spectra (HRMS) were obtained at the Technical Centre of Department of Synthetic Chemistry and Biological Chemistry of Kyoto University. The microscope observation was performed under crossed nicols using a Carl Zeiss AXIO IMAGER MIM polarising optical microscope (POM) equipped with a Linkam TH-600PM and L-600 heating and cooling stage with temperature control. The phase transition temperatures of the S_C and S_C* were determined using a Perkin-Elmer differential scanning calorimeter (DSC) and a TA instrument Q100 DSC apparatus at a constant heating and cooling rate of 2 °C/min by recording data for the first cooling and the second heating processes. X-ray diffraction (XRD) was performed using a Rigaku D-3F diffractometer equipped with a temperature controller under a constant heating and cooling rate of 1 °C/min, in which X-ray power was set at 12 kW.

3. Results and Discussion

The binaphthyl derivatives **D-3,3'**, **D-4,4'** and **D-6,6'** were synthesised by introducing the PCH-type LC groups into the 3,3', 4,4', and 6,6' positions of the binaphthyl ring, respectively, as depicted in Scheme 1. The synthetic routes for the binaphthyl derivatives are shown in Scheme 2. Compounds 2 and 5 were synthesised according to the literature.[12] Note that the ethoxy group at the 2,2' positions of the binaphthyl ring remains unchanged to reduce the number of relevant parameters when evaluating the effect of chirality transcription.[12]

(Scheme 1 and 2)

Chirality Transfer to N-LC

N*-LCs were prepared by adding small amounts of the binaphthyl derivatives as chiral dopants into 4-pentyl-4'-cyanobiphenyl (5CB) to be used as a host N-LC. All of the binaphthyl derivatives synthesised here showed good miscibility to the N-LC owing to PCH-type LC substituents. Figure 1 shows polarised optical microscope (POM) photographs of the N*-LCs induced by additions of 0.5 mol% **D-1**, **D-3,3'**, **D-4,4'** and **D-6,6'** to 5CB. Fingerprint textures were observed in the N*-LCs including **D-3,3'** (Figure 1b) and **D-6,6'** (Figure 1d). However, no fingerprint texture was found in the N*-LCs including **D-1** and **D-4,4'**. Nevertheless, the helical pitches of the N*-LCs were rigorously evaluated by measuring the distance between Cano lines appearing on the surface of a wedge-type cell under a POM.[12] The helical pitches of the N*-LCs with **D-1**, **D-3,3'**, **D-4,4'** and **D-6,6'** were 19.0, 1.9, 18.6 and 1.7 μm, respectively.

(Figure 1)

It is worth noting that the PCH substituents of the binaphthyl derivative allow the binaphthyl derivative to be miscible in the host N-LC, even at high binaphthyl derivative concentrations, such as 1 mol%. The change in helical pitch (p) of the N*-LC as a function of the mole percentage of the chiral dopant was examined. The HTP of the chiral dopant, i.e., its ability to convert N-LC into N*-LC, was evaluated using the equation

$$\mathrm{HTP} = [(1/p) / c]_{c \to 0}$$

where p is the helical pitch in μm and c is the mole fraction of the chiral dopant in the N*-LC. The HTPs of the n,n'-substituted binaphthyl derivatives (**D-3,3'**, **D-4,4'** and **D-6,6'**) and that of **D-1** are summarised in Table 1. The HTPs of the chiral dopants **D-3,3'** and **D-6,6'** have large HTPs of 153 and 154 μm^{-1}, respectively, which are approximately 14 times larger than that of **D-1** (HTP = 10.5). This difference can be attributed to the more efficient chirality transfer of **D-3,3'** and **D-6,6'** to the

environmental N-LC molecules through van der Waals intermolecular interactions between the PCH substituents of the chiral dopant and the cyanobiphenyl moiety of the N-LC relative to **D-1,** which has no PCH substituents.

(Table 1)

However, **D-4,4'** showed an unexpectedly small HTP value of 11 μm^{-1} despite having PCH substituents; the HTP value of **D-4,4'** is almost the same as that of **D-1**, 10.5 μm^{-1}. To explain this result, we examined the relationship between the HTP of the chiral dopant and the dihedral angle (θ) of LC substituents with respect to the axis of the binaphthyl ring. The dihedral angles were estimated from the equilibrium geometries calculated using the semi-empirical AM1 method. The estimated dihedral angles in **D-3,3'**, **D-4,4'** and **D-6,6'** were 60°, 0° and 60°, respectively. Thus, when the dihedral angle changed from $\theta = 0°$ (**D-4,4'**) to $\theta = 60°$ (**D-3,3'** and **D-6,6'**), the HTP of the binaphthyl derivative changed from 11 to 153-154 μm^{-1}, respectively. These results indicate that the substitution positions at 3,3' and 6,6' of the binaphthyl ring promote the transfer of the axial chirality of the binaphthyl derivative to the surrounding N-LC molecules.

The temperature dependence of the helical pitches in the N*-LCs was investigated by using the Cano wedge type cell. As shown in Figure 2, the helical pitches of the N*-LCs including D-3,3' and D-6,6' slightly increased with increasing temperature from 5 to 25 °C. In contrast, those of the N*-LCs including D-1 and D-4,4' showed no noticeable temperature dependence. These results suggest that the dihedral angle of the binaphthyl rings of D-3,3' and D-6,6' may become smaller owing to the increase in thermal motion of the chiral dopant, resulting in a slight decrease in helical twisting of the binaphthyl rings. The LC substituents at the 3,3' or 6, 6' positions of the binaphthyl rings should amplify the sensitivity of the helical twisting to the thermal motion.

Meanwhile, the LC substituents at the 4,4' positions of the binaphthyl rings are parallel to the helical axis at the 1, 1' positions and hence they do not effectively affect the twisting of the helical axis under the thermal motion. The negligibly small temperature dependence in D-4,4' is common

to D-1,1', where the large steric repulsion between hydrogens at the 8,8' positions of the binaphthyl rings restricts the internal rotation around the helical axis of 1,1' positions. [12,15]

(Figure 2)

Preparation of Smectic LCs

4-(4-Methylpentyloxy)phenyl-4-(decyloxy)benzoate [abbreviated as **PhB1**] and 4-(3-methylpentyloxy)phenyl-4-(decyloxy)benzoate [**PhB2**] were synthesised to prepare S_C-LCs (Scheme 3).[21] The mesomorphic properties of **PhB1** and **PhB2** were investigated using POM, DSC and XRD measurements. Figures 3a and 3b show DSC data for **PhB1** and **PhB2**, respectively. The phase transition temperatures of **PhB1** were K → 50 °C (87 J/g) → S_X → 72 °C (0.2J/g) → S_A → 76 °C (15 J/g) → I and I → 73 °C (18 J/g) → S_A → 69 °C (0.4 J/g) → S_C → 39 °C (13.1 J/g) → S_X → 6 °C (13.4 J/g) →K for the heating and cooling processes, respectively (Figure 3a). Meanwhile, the phase transition temperatures of **PhB2** were K → 50 °C (73 J/g) → S_A → 62.5 °C (11 J/g) → I and I → 62.2 °C (11.9 J/g) → S_A → 12.1 °C (5.3 J/g) → S_C → 5.3 °C (16.5 J/g) → K for the heating and cooling processes, respectively (Figure 3b). Here, K, S_C, S_A and I denote the crystal, smectic C, smectic A and isotropic phases, respectively, and the enthalpy changes associated with the phase transitions are given in parenthesis. The behaviours of the LC phase transitions in **PhB1** and **PhB2** were monotropic nature. POM photographs of **PhB1** and **PhB2** showed fan-shape textures characteristic of smectic phases at 50 °C and 40 °C in the cooling process, respectively (Figures 3c and 3d).

The XRD measurement of **PhB2** was performed during the cooling process (Figure 4c). At 55 °C, a broad diffraction peak was observed in the large-angle region (2θ = 19.8°), corresponding to the LC intermolecular distance of 4.5 Å. A sharp diffraction peak in the small-angle region (2θ = 2.8°) corresponds to an interlayer distance of d = 31.5 Å, which is similar to the molecular length of the **PhB2** (l = 30 Å). It follows that the LC phase of **PhB2** at 55 °C can be assigned to the

smectic A (S_A) phase. When cooled from 55 °C to 42 °C, the interlayer distance decreased from 31.5 to 23 Å. The d / l ratio of 0.77 implies that the tilted structure is formed, yielding the S_C phase. The tilt angle (α) defined between the layer normal and the director of LC molecules was calculated to be 40° from the equation $\alpha = \cos^{-1}(d / l)$. The schematic representations of the S_A and S_C phases of **PhB2** are shown in Figure 4b.

(Scheme 3, Figures 3 and 4)

Chirality Transfer in S_C-LCs

The binaphthyl derivatives of **D-1**, **D-3,3'**, **D-4,4'** and **D-6,6'** were added as chiral dopants into the S_C-LC of **PhB1**. As a result, the chiral dopanats of **D-3,3'** and **D-6,6'** only gave rise to chiral smectic C (S_C*) phases, where the typical helical pitches were 4.4 and 1.6 μm, respectively, when 1.0 mol% chiral dopnats were used (see Table 2). As shown in Figure 5, the mesomorphic properties of **PhB1** including **D-6,6'** [abbreviated as **PhB1–D-6,6'**] were investigated in more details by using DSC and POM measurements. The DSC thermographs of **PhB1** with 1 mol% of **D-6,6'** were obtained with heating and cooling rates of 2 °C/min. The phase transition temperatures of **PhB1–D-6,6'** were K→ 50 °C (70.4 J/g) → S_X → 60 °C (0.2 J/g) → S_C* → 67 °C (0.003 J/g)→ S_A → 75 °C (10.1 J/g) → I and I → 73 °C (13.0 J/g) → S_A → 68 °C (0.09 J/g) → S_C* → 55 °C (0.3 J/g) → S_{X1} → 38 °C (11.2 J/g) → S_{X2} → 7 °C (14.8 J/g) → K for the heating and cooling processes, respectively (Figure 5a). The POM photographs of **PhB1–D-6,6'** were taken during the heating and cooling processes. The striated fan-shape textures, observed at 64 °C in the heating (Figure 5b) and at 66 °C in the cooling (Figure 5c) process, were assigned as the S_C* phase. The results indicate that the S_C*-LC induced in **PhB1–D-6,6'** has an enantiotropic nature. The POM photographs also show that there exist S_X phase with finger-print texture and S_A phase with fan-shaped one at lower and higher temperature region of the S_C* phase, respectively.

(Figure 5)

Figure 6 shows POM photographs of the **PhB2** including 1 mol% of **D-1**, **D-3,3'**, **D-4,4'** and **D-6,6'**, respectively. The POM photographs of **PhB2–D-1** and **PhB2–D-4,4'** showed fan-shape textures characteristic of the S_A phase at 30 °C and 50 °C during the cooling processes, respectively (Figure 6a and 6c). When the chiral dopants of **D-3,3'** and **D-6,6'** were used, the striated fan-shape textures were observed at 35 °C (Figure 6b and 6d).

(Figure 6)

As shown in Figure 7a, DSC indicates that **PhB2–D-6,6'** has a monotropic S_C* phase. Namely, the Sc* phase was observed only on cooling process. This is in contrast to the case of **PhB1–D-6,6'** with enantiotropic S_C* phase. The phase transition temperatures of **PhB2–D-6,6'** were K → 50 °C (78.2 J/g) → S_X → 54 °C → S_A → 62 °C (9.9 J/g) → I and I → 59 °C (6.0 J/g) → S_A → 29 °C → S_C* → 22 °C → S_{X1} → 9 °C (3.4 J/g) → S_{X2} → 5 °C (9.7 J/g) → K during the heating and cooling processes, respectively. The phase transitions and the enthalpy changes in **PhB2–D-1**, **PhB2–D-3,3′**, **PhB2–D-4,4′** and **PhB2–D-6,6′** are also shown in Figure 8. Figure 7b depicts the XRD patterns of **PhB2–D-6,6'** at 50 °C and 27 °C during the cooling process. The XRD at 50 °C exhibited a sharp diffraction peak in the small-angle region ($2\theta = 2.7°$), corresponding to an interlayer distance of $d = 32.7$ Å. From the XRD and POM results, the LC phase of **PhB2–D-6,6'** at 50 °C was assigned as the S_A phase. When cooled to 27 °C, the diffraction peak was observed at an angle of 4.4° in 2θ ($d = 20$ Å). Moreover, a sharp diffraction peak was observed in the wide angle region at 22° in 2θ, which corresponds to the LC intermolecular distance of 4 Å (Figure 7C). The ratio (d / l) between the interlayer distance (d) and the molecular length (l) was 0.67, suggesting that the LC molecules form a tilted structure. The tilt angle between the layer normal and the director of the LC molecules was estimated to be 48°. Thus, the LC phase of

PhB2–D-6,6' at 27 °C was assigned as the S_C* phase. The helical structure in the S_C* phase is represented by a precession of the director *n* around the layer normal *z*, where the azimuth angle is kept constant (see the picture at the left site in Figure 7c).

(Figures 7 and 8)

The helical pitch of the S_C* phase was estimated by directly measuring the distances between the striated lines of the optical texture in POM.[1,22] The results are summarized in Table 2. The S_C* phases of **PhB2** induced by the chiral dopants (1 mol%) of **D-3,3'** and **D-6,6'** showed helical pitches of 3.7 μm and 1.4 μm, respectively (see also Figures 6b and 6d). Considering these results, the latter (**D-6,6'**) is more promising for the transfer of the axial chirality of the binaphthyl derivative to the surrounding host LC molecules of **PhB2**. The favourableness of **D-6,6'** as the chiral dopant giving highly twisted S_C* phase also holds for **PhB1** (Table 2).

Subsequently, the dependence of the helical pitch on the concentration of the chiral dopant was examined in the S_C*-LCs of **PhB1–D-6,6'** and **PhB2–D-6,6'**, for which the S_C* temperatures at 60 and 27 °C were used, respectively. As depicted in Figure 9, the helical pitches varied from 4.0 to 1.4 μm for mole percentages from 0.5 to 1.5 mol% for **D-6,6'** in **PhB1**, while those from 4.3, 2.75 to 1.2 μm for mole percentages from 0.375, 0.4 to 1.5 mol% for **D-6,6'** in **PhB2**. It is evident that **PhB2** forms a higher twisted helical S_C*-LC with less amount of **D-6,6'** than **PhB1**. In addition, **PhB2** shows a remarkable decrease in helical pitch (increase in helical twisting) even when small amounts of chiral dopant is added, implying that **PhB2** can more easily form the induced S_C*-LC upon the addition of the chiral dopant than **PhB1**.

(Table 2, Figure 9)

Finally, it is worth noting that tilt angle (θ) in the S_C*-LC is estimated to 48° as depicted in Figure 7c, and this value is larger than that (48) in the S_C-LC (Figure 3b). Namely, the tilt angle of

the S_C-LC increased by 8° when the chiral dopant, **D-6,6'** was added into the host LC, **PhB2,** to form the S_C*-LC. It is likely that, upon the addition of the chiral dopant, the LC molecules in S_C phase are rearranged by the precessing motion about the layer normal to avoid the steric repulsion incurred by the chiral dopants, generating a one-handed screwed S_C* phase. This rearrangement could be easier when the tilt angle is larger because of the larger motional spacing for the LC molecules. This remark may lead to a guideline for designing the LC molecules that can be used as the host S_C-LCs producing the induced S_C* phase with an aid of the chiral dopants.

4. Conclusion

We synthesised novel atropisomeric chiral inducers, axially chiral binaphthyl derivatives bearing LC groups at the *n*,*n*' positions (*n* = 3, 4, 6) of the binaphthyl rings. The chirality transfer from the axially chiral binaphthyl derivatives to the N-LC molecules was largely affected by the dihedral angle of LC groups with respect to the chiral axis of the binaphthyl moiety. When the LC groups were introduced at the 3,3' and 6,6' positions of the binaphthyl rings, the dihedral angle became 60°, leading to high HTPs of 153 and 154 μm^{-1}, respectively. In contrast, when the LC groups were substituted at the 4,4' position of the binaphthyl rings, the dihedral angle became 0°, resulting in a small HTP of 11 μm^{-1}. The substituents at the 3,3' and 6,6' positions of the binaphthyl rings are effective in the chirality transfer of the chiral dopant to the environmental N-LC molecules.

The S_C* phases were induced when the dopant, **D-3,3'** or **D-6,6'** was added to the host LC, **PhB1** and **PhB2**. This means that it is possible to not only induce the S_C*-LC by using the chiral dopants and the host LCs, but also tune the helical pith of the S_C*-LC by choosing the combination between the chiral dopant and the host LC. In particular, the highly twisted S_C* phases with helical pitches of 1.2 ~ 1.4 μm were prepared in **PhB1** and **PhB2** by using the chiral dopant of **D-6,6'**.

The 6,6' positions of binaphthyl rings are the optimal substitution positions for achieving the chirality transfer effectively from the axially chiral binaphthyl moieties to the N- and S_C-LCs.

This comprehensive study of the optimal substitution position of axially chiral binaphthyl derivatives for effective chirality transfer might lead to the molecular designs of other atropisomers and even chiroptical materials.

Acknowledgement: This work was supported by a Grant-in-Aid for Science Research (S) (No. 20225007) from the Ministry of Education, Culture, Sports, Science and Technology, Japan. The authors also acknowledge the Korea Institute of Science and Technology Institutional program.

References

1 (*a*) J. W. Goodby, *J. Mater. Chem.*, 1991, **1**, 307-318; (*b*) H. S. Kitzerow and C. Bahr, *Chirality in Liquid Crystals*, Springer, New York, 2000; (*c*) S. Pieraccini, S. Masiero, A. Ferrarini and G. P. Spada, *Chem. Soc. Rev.*, 2011, **40**, 258-271.

2 G. Solladie and R. G. Zimmermann, *Angew. Chem., Int. Edit.,* 1984, **23**, 348-362.

3 R. P. Lemieux, *Chem. Soc. Rev.*, 2007, **36**, 2033-2045.

4 (*a*) D. Coates and G. W. Gray, *Phys. Lett. A.*, 1973, **45A**, 115-116; (*b*) M. Lee, S. T. Hur, H. Higuchi, K. Song, S. W. Choi and H. Kikuchi, *J. Mater. Chem.*, 2010, **20**, 5813-5816.

5 (*a*) S. R. Renn and T. C. Lubensky, *Phys. Rev. A.*, 1988, **38**, 2132-2147; (*b*) J. W. Goodby, M. A. Waugh, S. M. Stein, E. Chin, R. Pindak and J. S. Patel, *Nature*, 1989, **337**, 449-452; (*c*) G. Srajer, R. Pindak, M. A. Waugh, J. W. Goodby and J. S. Patel, *Phys. Rev. Lett.*, 1990, **64**, 1545-1548.

6 J. W. Goodby, I. Nishiyama, A. J. Slaney, C. J. Booth and K. J. Toyne, *Liq. Cryst.*, 1993, **14**, 37-66.

7 S. Pieraccini, M. I. Donnoli, A. Ferrarini, G. Gottarelli, G. Licini, C. Rosini, S. Superchi and G. P. Spada, *J. Org. Chem.*, 2003, **68**, 519-526.

8 R. P. Lemieux, *Acc. Chem. Res.*, 2001, **34**, 845-853.

9 (*a*) H. G. Kuball and H. Bruning, *Chirality*, 1997, **9**, 407-423; (*b*) D. Vizitiu, C. Lazar, B. J Halden and R. P. Lemieux, *J. Am. Chem. Soc.*, 1999, **121**, 8229-8236; (*c*) H. G. Kuball, *Liq. Cryst. Today*, 1999, **9**, 1-7.

10 A. Januszko, P. Kaszynski and W. Drzewinski, *J. Mater. Chem.*, 2006, **16**, 452-461.

11 A. Yoshizawa, K. Kobayashi and M. Sato, *Chem. Comm.*, 2007, 257-259.

12 (*a*) M. Goh, M. Kyotani and K. Akagi, *J. Am. Chem. Soc.*, 2007, **129**, 8519-8527; (*b*) M. Goh and K. Akagi, *Liq. Cryst*., 2008, **35**, 953-965.

13 (*a*) A. J. Slaney, I. Nishiyama, P. Styring and J. W. Goodby, *J. Mater. Chem*., 1992, **2**, 805-810; (*b*) H. G. Kuball, T. Muller and H. G. Weyland, *Mol. Cryst. Liq. Cryst*. 1992, **215**, 271-278; (*c*) M. Goh, T. Matsushita, M. Kyotani and K. Akagi, *Macromolecules*, 2007, **40**, 4762-4771.

14 (*a*) K. Ichimura, *Chem. Rev.*, 2000, **100**, 1847-1873; (*b*) T. Ikeda, *J. Mater. Chem.*, 2003, **13**, 2037-2057; (*c*) H. Akiyama, A. Tanaka, H. Hiramatsu, J. Nagasawa and N. Tamaoki, *J. Mater. Chem.*, 2009, **19**, 5956-5963; (*d*) R. Eelkema, M. M. Pollard, J. Vicario, N. Katsonis, B. S. Ramon, C. W. M. Bastiaansen, D. J. Broer and B. L. Feringa, *Nature*, 2006, **440**, 163-163; (*e*) H. Hayasaka, T. Miyashita, M. Nakayama, K. Kuwada and K. Akagi, *J. Am. Chem. Soc.,* 2012, **134**, 3758-3765.

15 (*a*) K. Akagi, G. Piao, S. Kaneko, K. Sakamaki, H. Shirakawa and M. Kyotani, *Science*, 1998, **282**, 1683-1686; (*b*) K. Akagi, S. Guo, T. Mori, M. Goh, G. Piao and M. Kyotani, *J. Am. Chem. Soc*., 2005, **127**, 14647-14654; (*c*) K. Akagi, *Chem. Rev.,* 2009, **109**, 5354-5401; (*d*) M. Goh, S. Matsushita and K. Akagi, *Chem. Soc. Rev.,* 2010, **39**, 2466-2476; (*e*) T. Mori, M. Kyotani and K. Akagi, *Chem. Sci.,* 2011, **2**, 1389-1395.

16 (*a*) N. L. Kramarenko, V. I. Kulishov, L. A. Kutulya, G. P. Semenkova, V. P. Seminozhenko and N. I. Shkolnikova, *Liq. Cryst.*, 1997, **22**, 535; (*b*) I. Dierking, *Liq. Cryst.*, 2001, **28**, 165.

17 (*a*) P. J. M. Pelaez, Y.S. Uh, C. Lata, M. P. Thompson, R. P. Lemieux and C. M. Crudden, *J. Org. Chem*., 2006, **71**, 5921-5929; (*b*) L. Pu, *Chem. Rev.* 1998, **98**, 2405-2494.

18 (*a*) G. Gottarelli, M. Hibert, B. Samori, G. Solladie, G. P. Spada and R. Zimmermann, *J. Am. Chem. Soc*., 1983, **105**, 7318-7321; (*b*) J. Rokunohe and A. Yoshizawa, *J. Mater. Chem.*, 2005, **15**, 275-279; (*c*) G. Heppke, D. Lotzsch and F. Oestreicher, *Z. Naturforsch.*,

1986, **41**, 1214-1218; (*d*) Q. Li, L. Green, N. Venkataraman, I. Shiyanovskaya, A. Khan, A. Urbas and J. W. Doane, *J. Am. Chem. Soc*., 2007, **129**, 12908-12909.

19 (*a*) H. J. Deussen, P. V. Shibaev, R. Vinokur, T. Bjornholm, K. Schaumburg, K. Bechgaard and V. P. Shibaev, *Liq. Cryst.*, 1996, **21**, 327-340; (*b*) K. Kanazawa, I. Higuchi and K. Akagi, *Mol. Cryst. Liq. Cryst.*, 2001, **364**, 825-834.

20 R. A. van Delden, T. Mecca, C. Rosini and B. L. Feringa, *Chem. Eur. J.*, 2004, **10**, 61-70.

21 M. P. Thompson and R. P. Lemieux, *J. Mater. Chem.*, 2007, **17**, 5068-5076.

22 K. Kobayashi and A. Yoshizawa, *Mol. Cryst. Liq. Cryst.*, 2009, **509**, 955-964.

Captions

Scheme 1. Molecular structures of axially chiral binaphthyl derivatives (**D-1**, **D-3,3'**, **D-4,4'** and **D-6,6'**) and host liquid crystals (**5CB**, **PhB1** and **PhB2**).

Scheme 2. Synthetic routes for axially chiral binaphthyl derivatives (**D-3,3'**, **D-4,4'** and **D-6,6'**).

Scheme 3. Synthetic routes for 4-(3-methylpentyloxy)phenyl-4-(decyloxy)benzoate (**PhB2**).

Figure 1. Polarising optical micrographs of N*-LCs induced by additions of 0.5 mol% of (a) **D-1**, (b) **D-3,3'**, (c) **D-4,4'** and (d) **D-6,6'** into the host N-LC of 5CB. The photographs of (a), (b) and (c) were taken at 28 °C during the cooling processes. The photograph of (d) was taken at 30 °C during the cooling process.

Figure 2. Temperature dependence of the helical pitches in the N*-LCs induced by addition of 0.5 mol% of the chiral dopants (**D-1**, **D-3,3′**, **D-4,4′** and **D-6,6′**) into 5CB.

Figure 3. Differential scanning calorimetry (DSC) thermographs and polarising optical microscope (POM) photographs of the host S_C-LCs, **PhB1** and **PhB2**. The DSC thermographs (a) **PhB1** and (b) **PhB2** were obtained with a constant heating and cooling rate of 2 °C/min. The POM photographs of **PhB1** (c, d) and **PhB2** (e, f) were taken during the heating and cooling processes, respectively.

Figure 4. (a) X-ray diffraction (XRD) profiles of **PhB2** measured in the cooling process. (b) Schematic illustration of the molecular arrangements in the S_C (left) and S_A (right) phases **PhB2**. *z*: layer normal, *n*: director.

Figure 5. DSC thermographs and POM photographs of the host S_C-LC, **PhB1** with 1 mol% of **D-6,6'**. The DSC thermographs (a) **PhB1** with 1 mol% of **D-6,6'** were obtained with heating and cooling rates of 2 °C/min. The POM photographs of **PhB1** with 1 mol% of **D-6,6'** were taken during the heating (b) and cooling (c) processes.

Figure 6. POM photographs of (a, c) S_A and (b, d) S_C* phases induced by the addition of 1 mol% of (a) **D-1**, (b) **D-3,3'**, (c) **D-4,4'** and (d) **D-6,6'** into the host S_C-LCs of **PhB2**.

Figure 7. (a) DSC thermograph and (b) XRD profiles of **PhB2** with 1 mol% of **D-6,6'**. XRD diffractions were measured during the cooling process. (c) Schematic illustration of the molecular arrangements in the S_C* and S_A phases.

Figure 8. The phase transition temperatures (°C) and transition enthalpies [ΔH (J/g)] (measured on cooling and heating rate of 2 °C/min) of **PhB2–D-1**, **PhB2–D-3,3′**, **PhB2–D-4,4′** and **PhB2–D-6,6′**.

Figure 9. Changes in the helical pitch of S_C* as a function of the mole percentage of the chiral dopant **D-6,6'** added into the host LC, **PhB1 and PhB2**.

Table 1. Specific rotation and helical twisting powers of axially chiral binaphthyl derivatives.

Table 2. Helical pitches of S_C* phases induced between host LCs and chiral dopants.

Chiral dopants

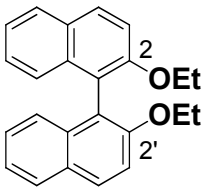

D-1

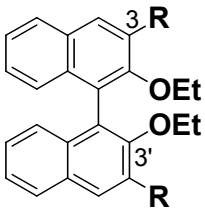

D-3,3'

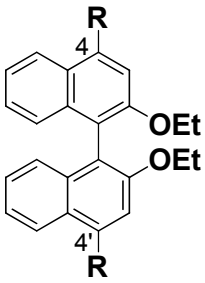

D-4,4'

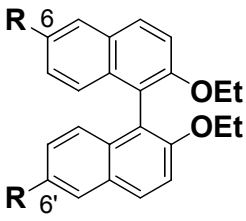

D-6,6'

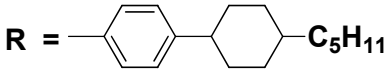

N-LC

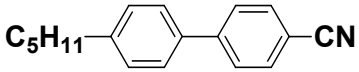

5CB

S_C

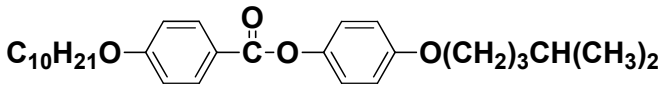

PhB1

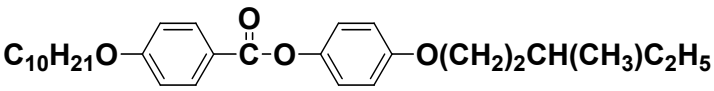

PhB2

Scheme 1. Molecular structures of axially chiral binaphthyl derivatives (**D-1**, **D-3,3'**, **D-4,4'** and **D-6,6'**) and host liquid crystals (**5CB**, **PhB1** and **PhB2**).

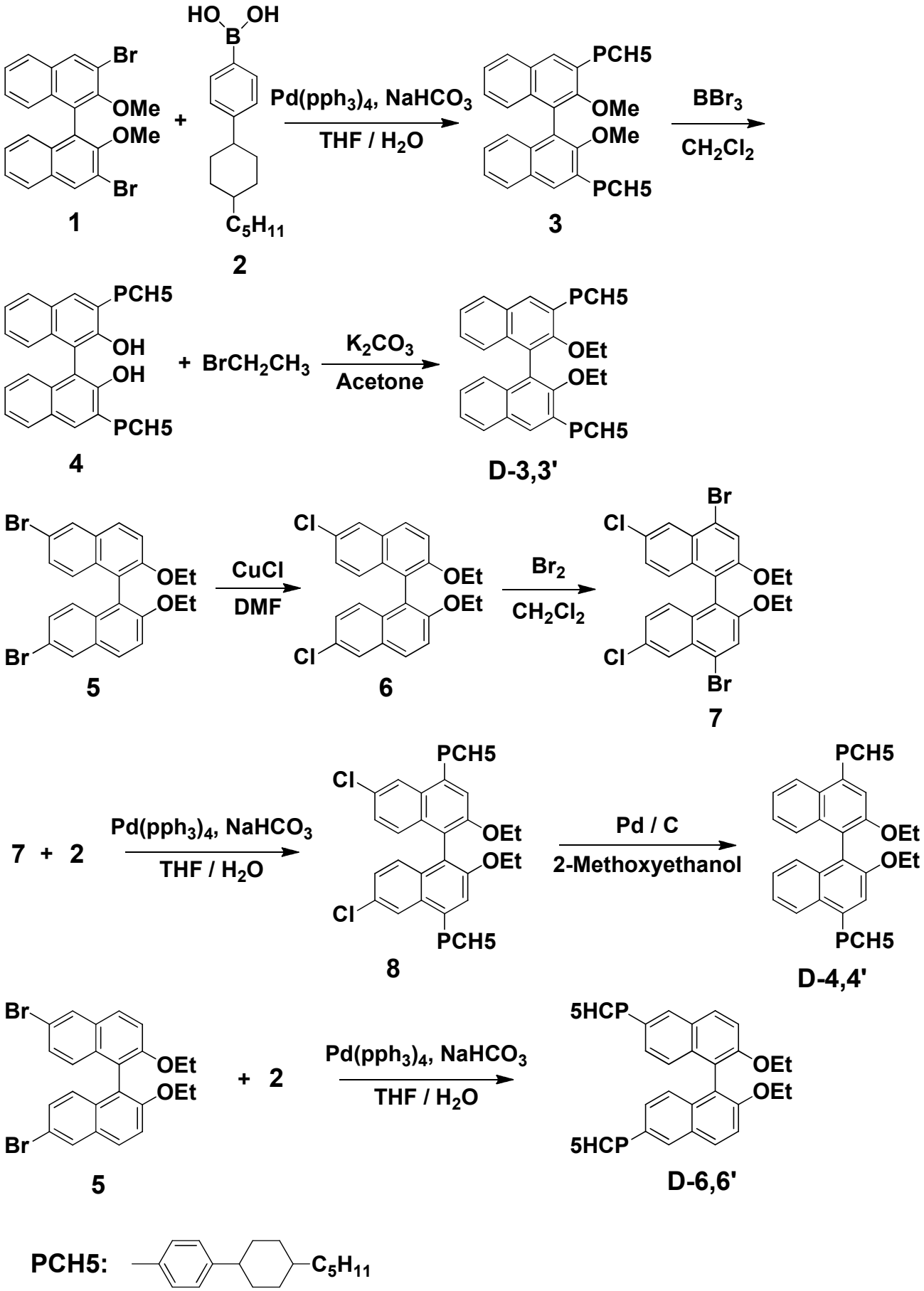

Scheme 2. Synthetic routes for axially chiral binaphthyl derivatives (**D-3,3'**, **D-4,4'** and **D-6,6'**).

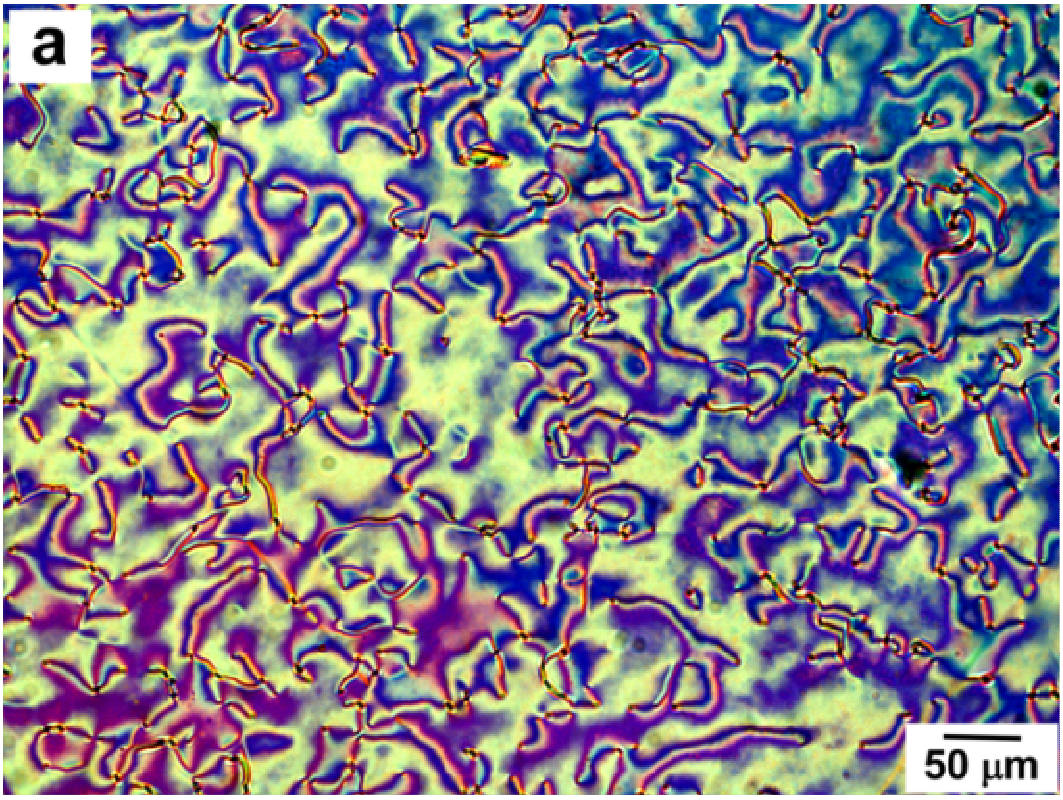

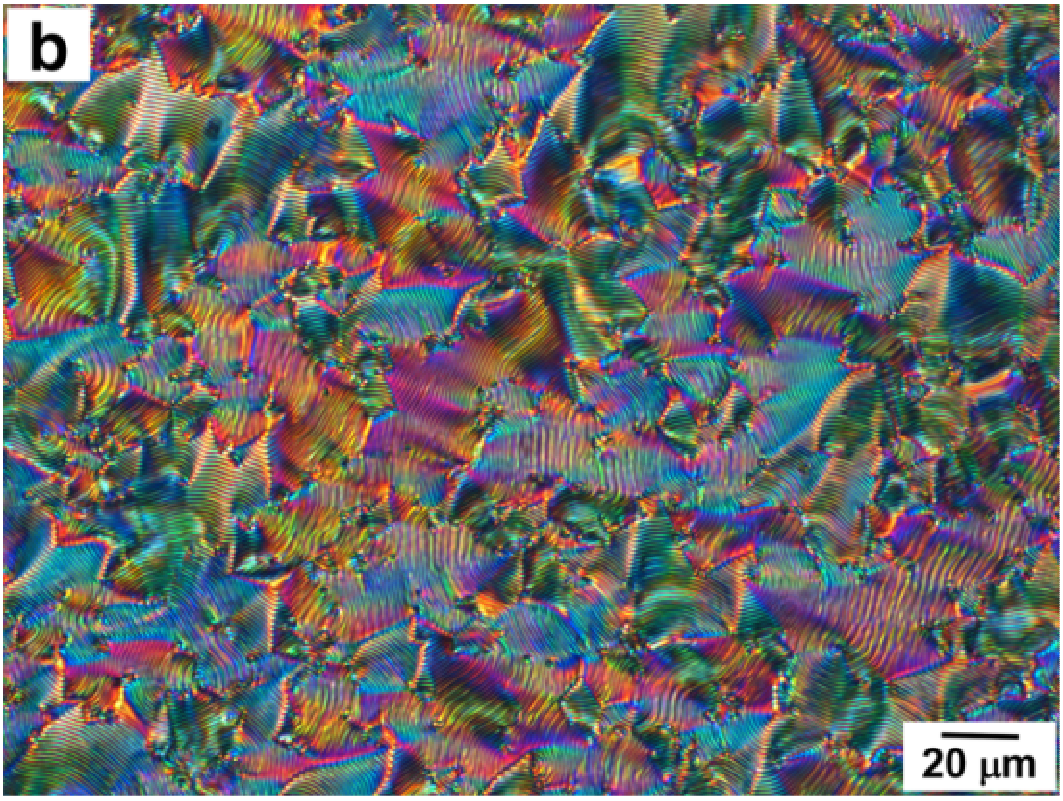

Continued

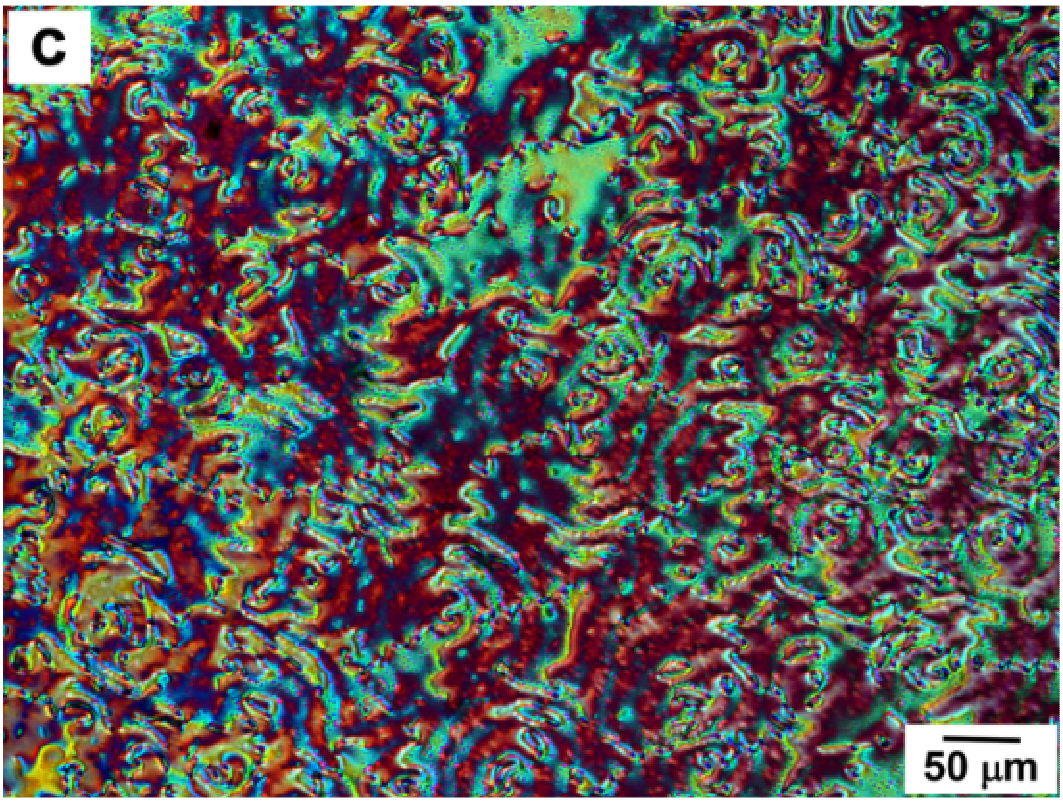

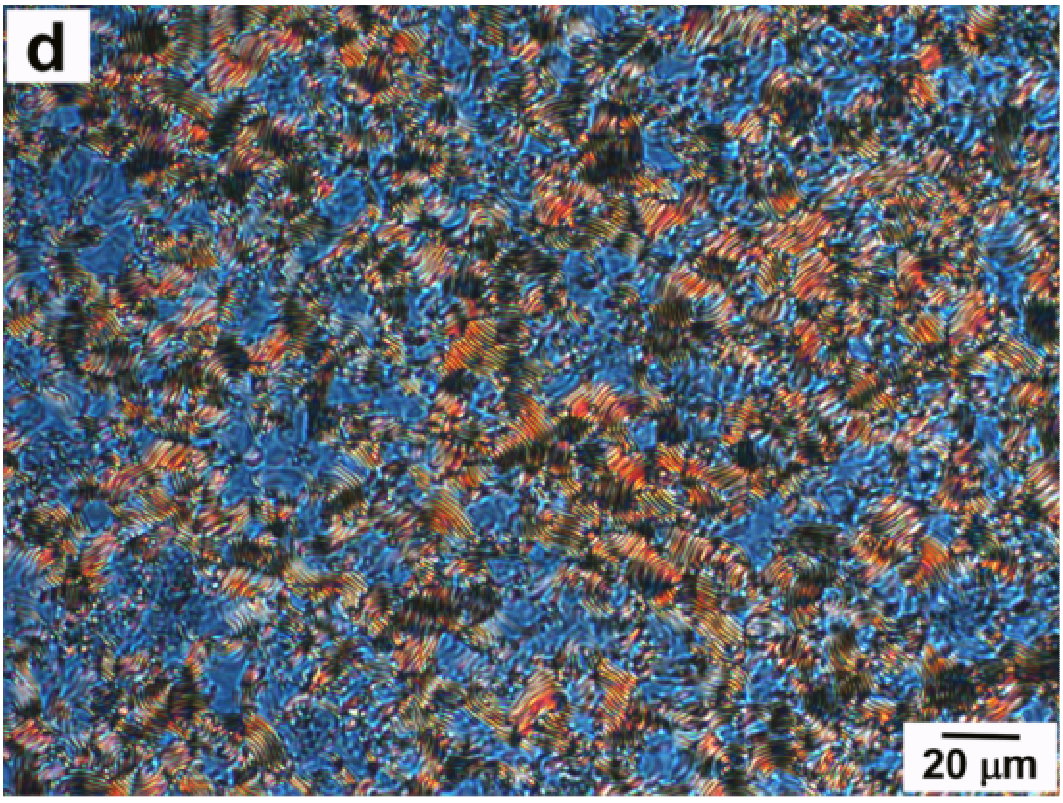

Figure 1. Polarising optical micrographs of N*-LCs induced by additions of 0.5 mol% of (a) **D-1**, (b) **D-3,3'**, (c) **D-4,4'** and (d) **D-6,6'** into the host N-LC of 5CB. The photographs of (a), (b) and (c) were taken at 28 °C during the cooling processes. The photograph of (d) was taken at 30 °C during the cooling process.

Table 1. Specific rotation and helical twisting powers of axially chiral binaphthyl derivatives.

	Specific rotation, $[\alpha]^{25}_{589}$, (deg·dm^{-1}·g^{-1}·cm^{3})	Helical twisting power (μm^{-1})
D-1	+ 6.5	10.5
D-3,3'	– 25.3	153
D-4,4'	+ 10.7	11
D-6,6'	– 24.3	154

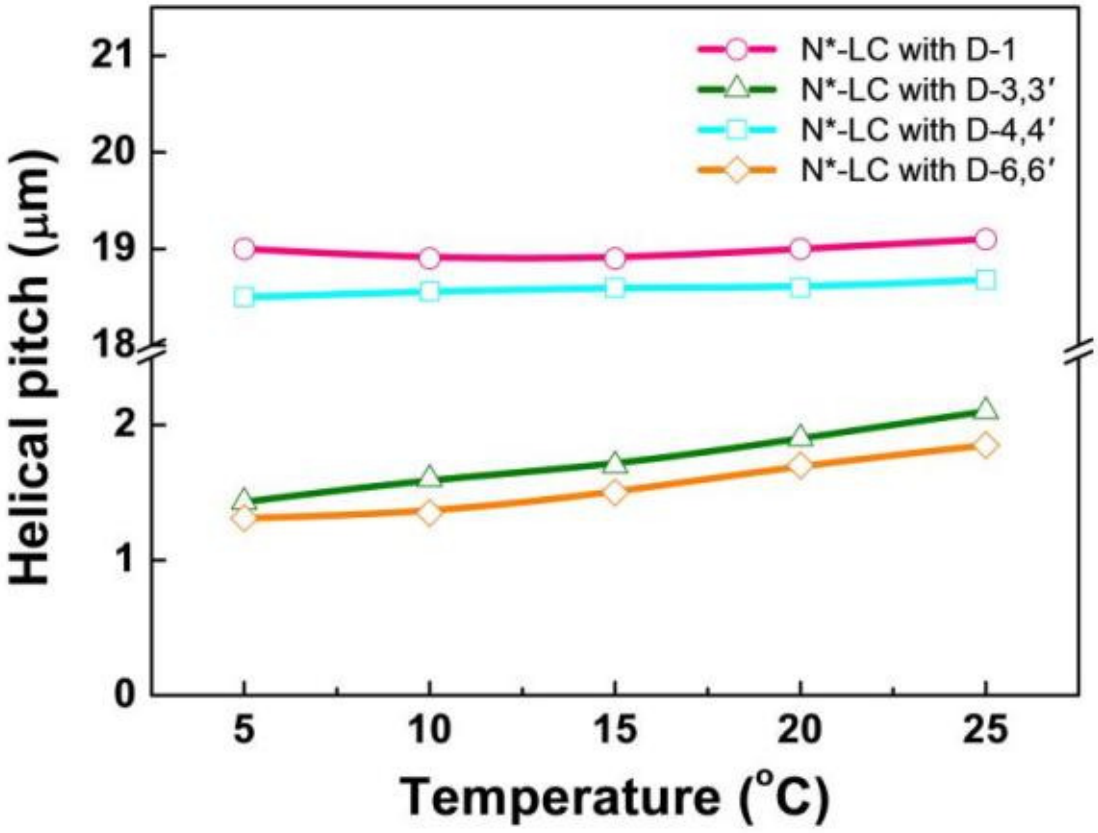

Figure 2. Temperature dependence of the helical pitches in the N*-LCs induced by addition of 0.5 mol% of the chiral dopants (**D-1**, **D-3,3′**, **D-4,4′** and **D-6,6′**) into 5CB.

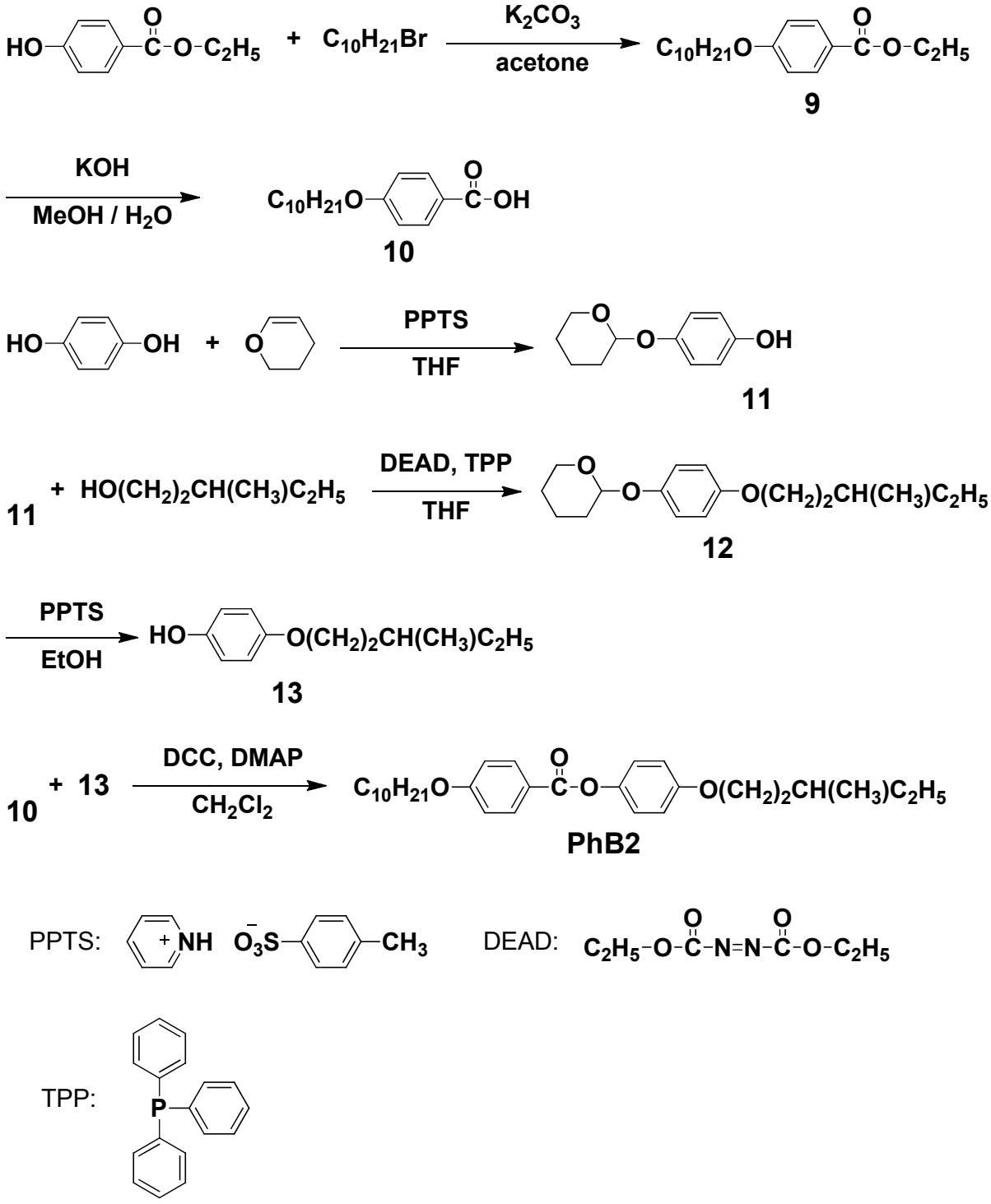

Scheme 3. Synthetic routes for 4-(3-methylpentyloxy)phenyl-4-(decyloxy)benzoate (**PhB2**).

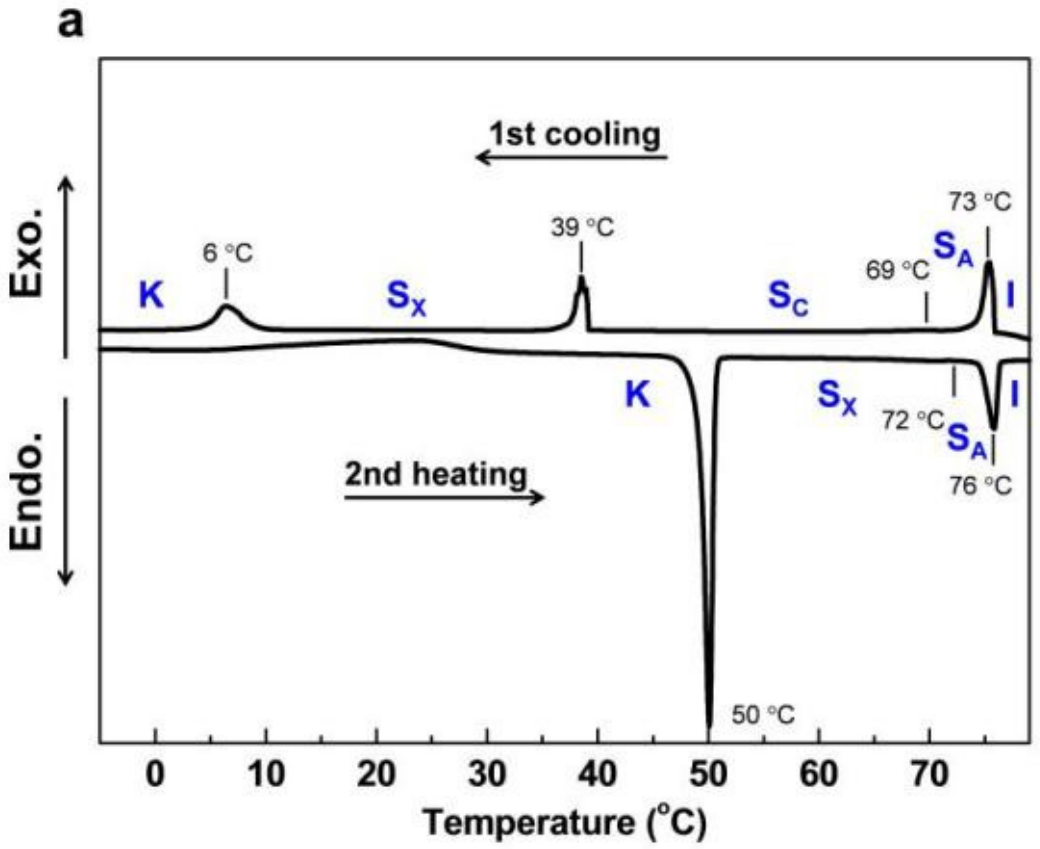

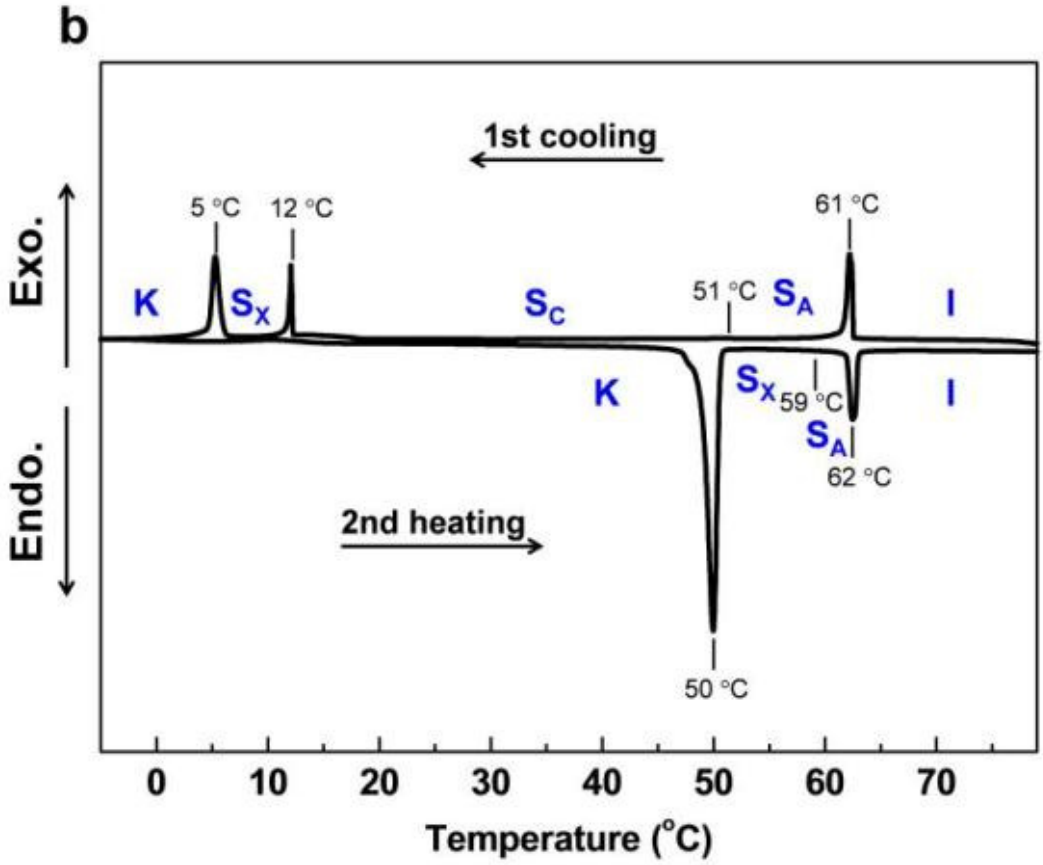

Continued

C

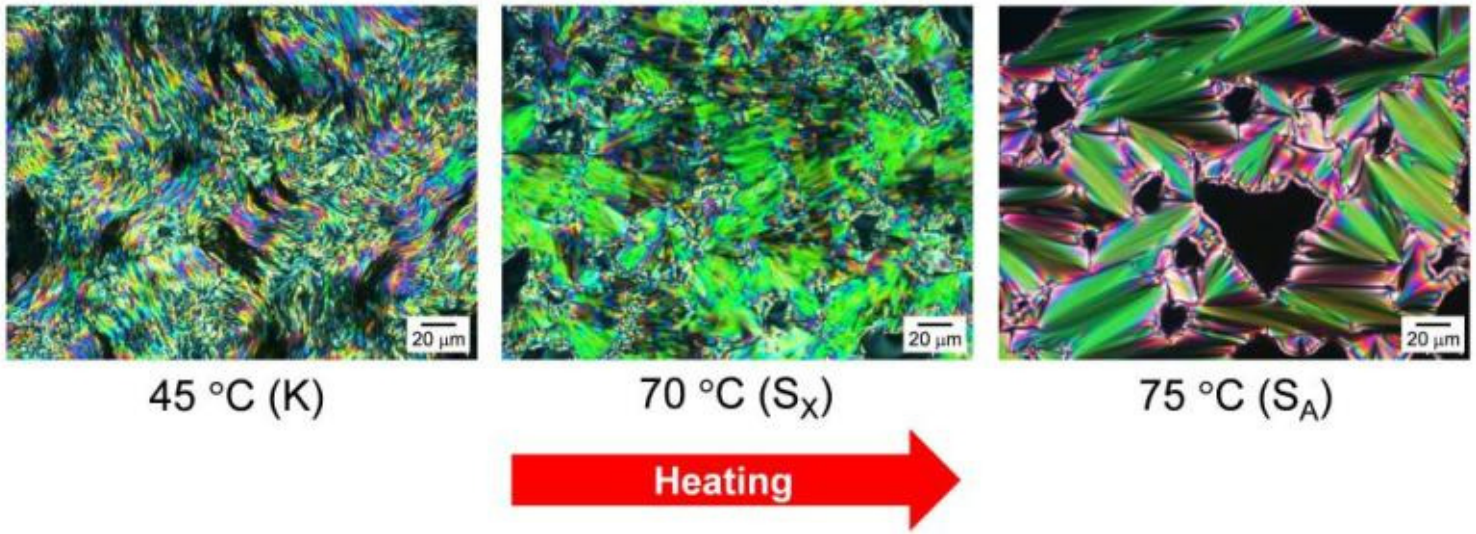

Continued

d

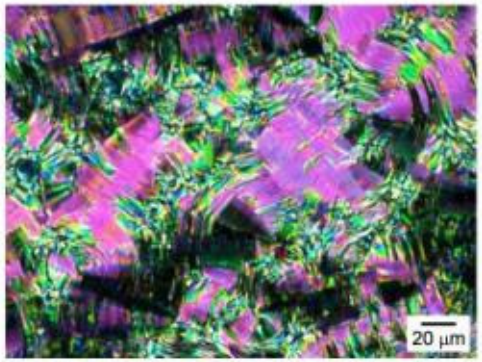

-5 °C (K)

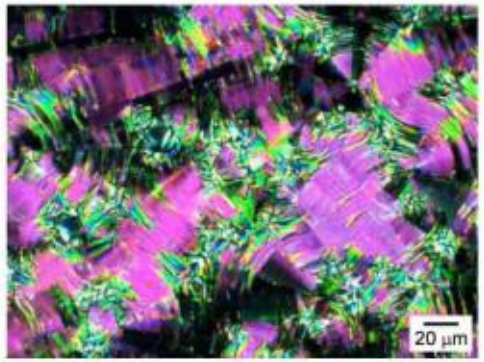

16 °C (S_X)

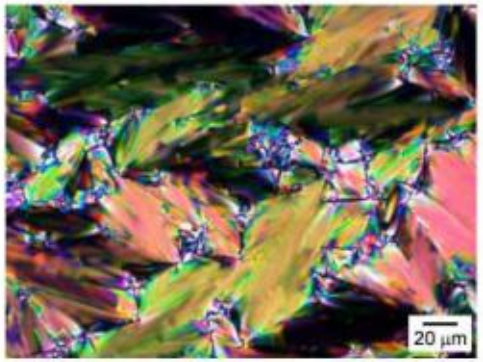

66 °C (S_C)

Cooling

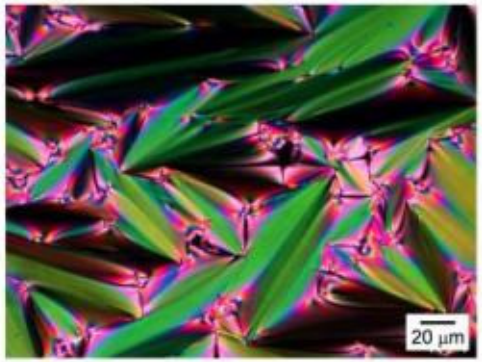

73 ° (S_A)

Continued

e

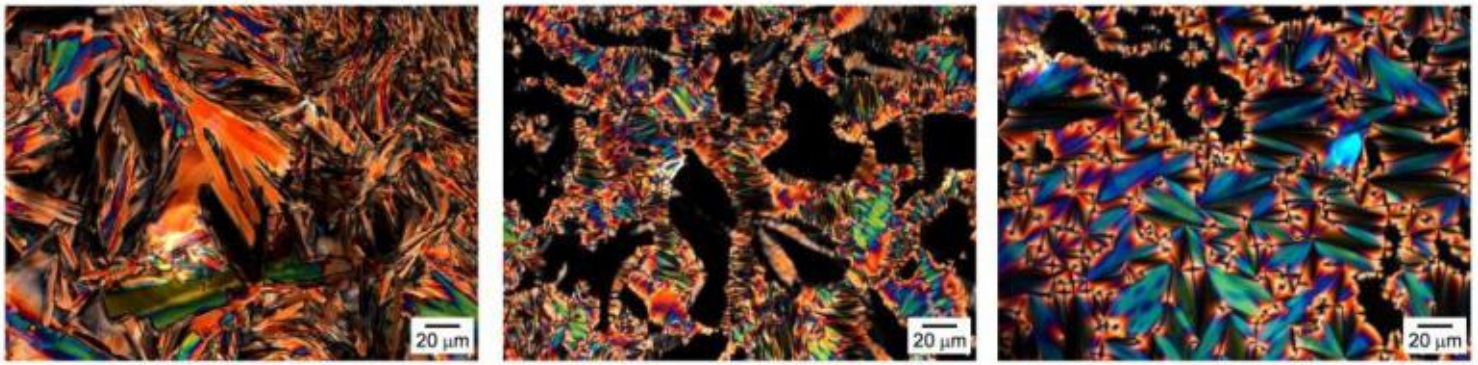

Continued

f

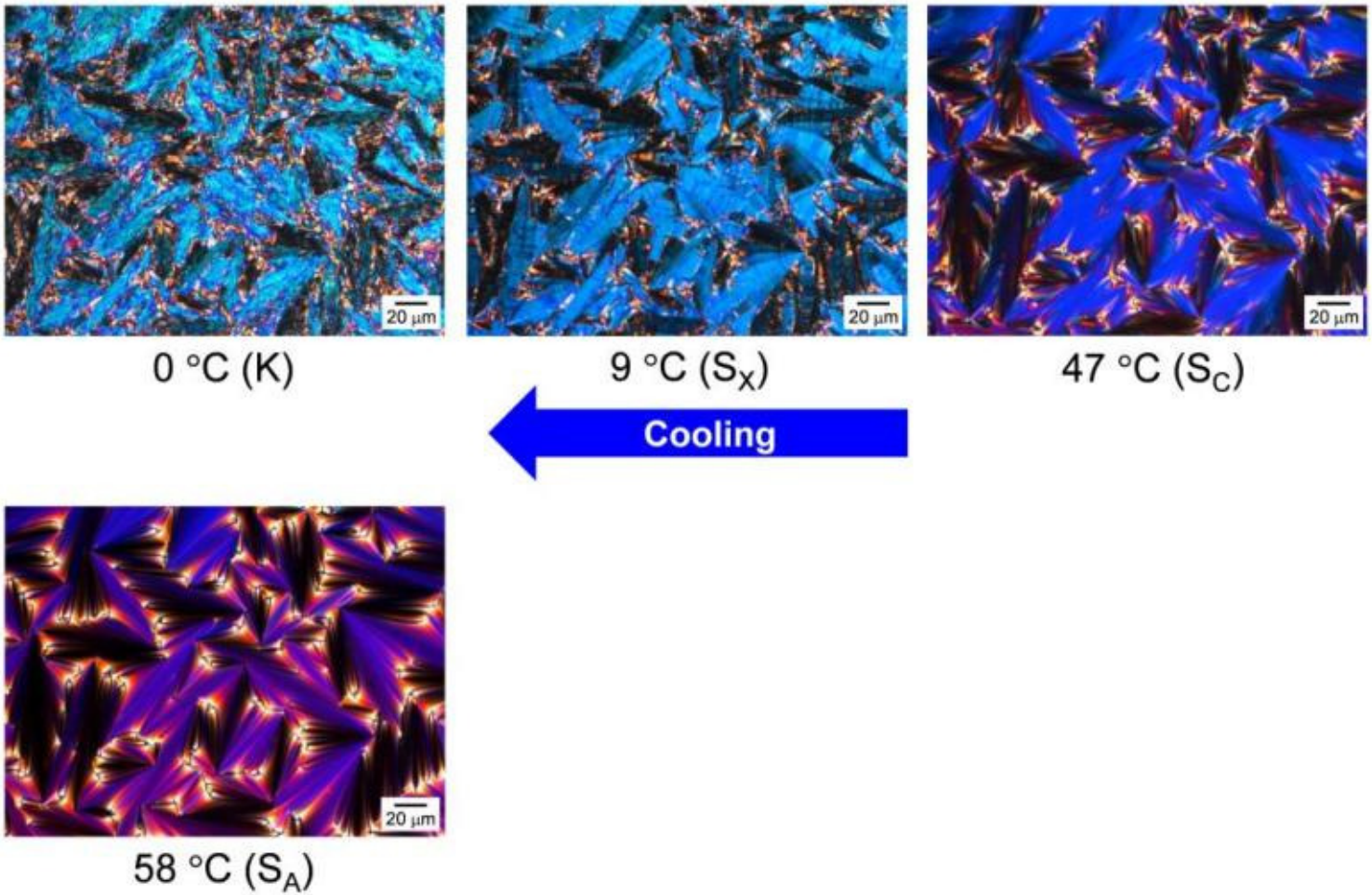

Figure 3. Differential scanning calorimetry (DSC) thermographs and polarising optical microscope (POM) photographs of the host S_C-LCs, **PhB1** and **PhB2**. The DSC thermographs (a) **PhB1** and (b) **PhB2** were obtained with a constant heating and cooling rate of 2 °C/min. The POM photographs of **PhB1** (c, d) and **PhB2** (e, f) were taken during the heating and cooling processes, respectively.

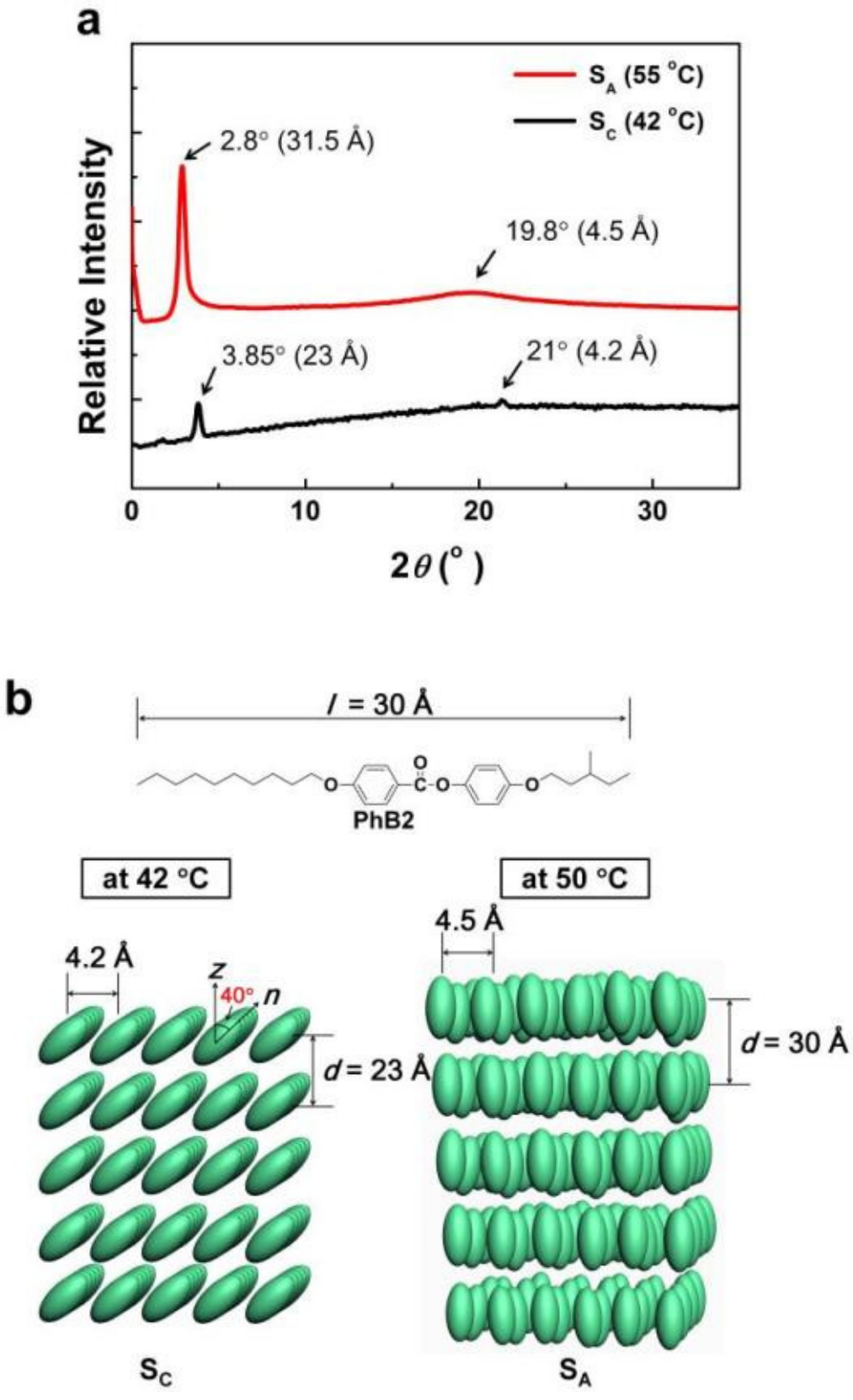

Continued

Figure 4. (a) X-ray diffraction (XRD) profiles of **PhB2** measured in the cooling process. (b) Schematic illustration of the molecular arrangements in the S_C (left) and S_A (right) phases **PhB2**. *z*: layer normal, *n*: director.

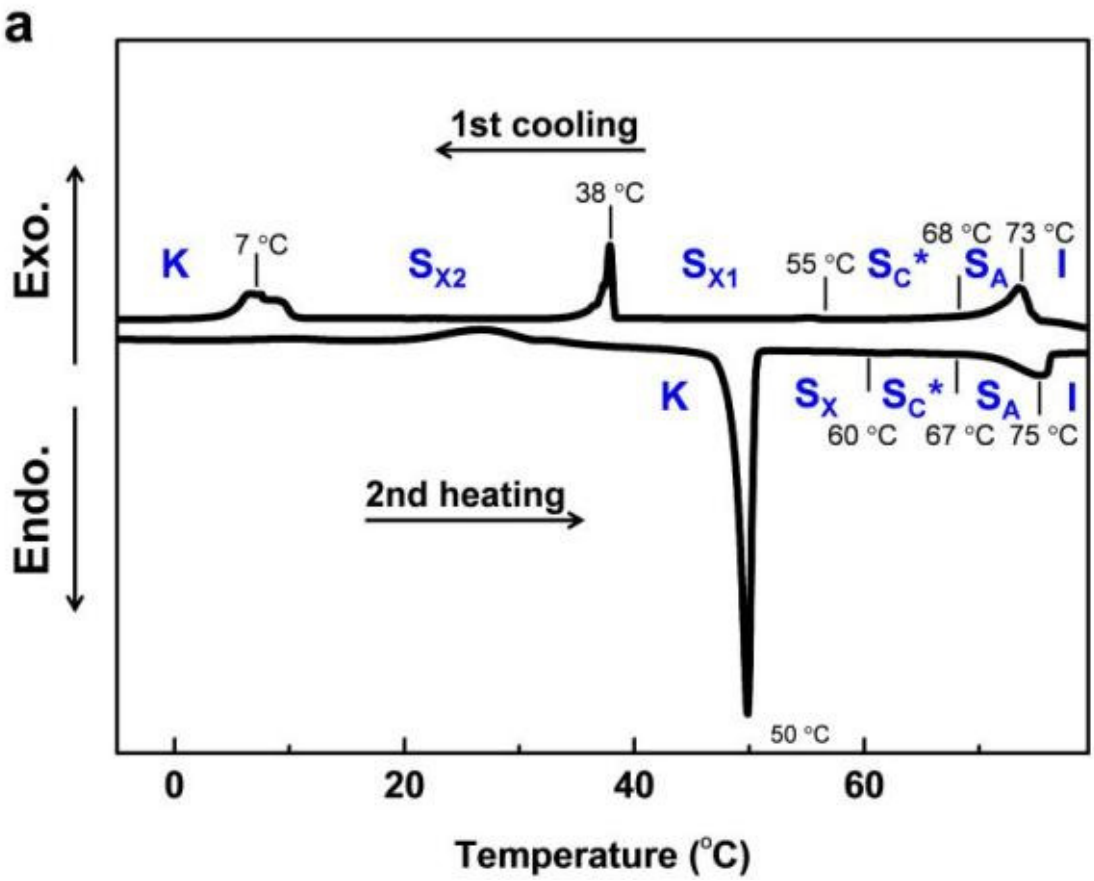

Continued

b

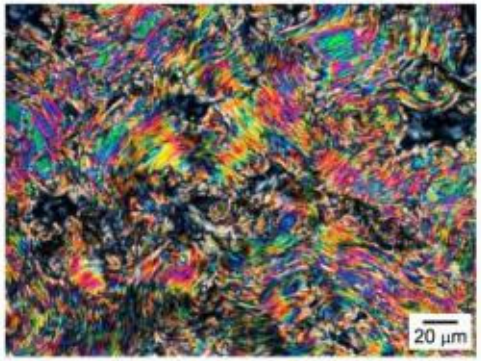

44 °C (K)

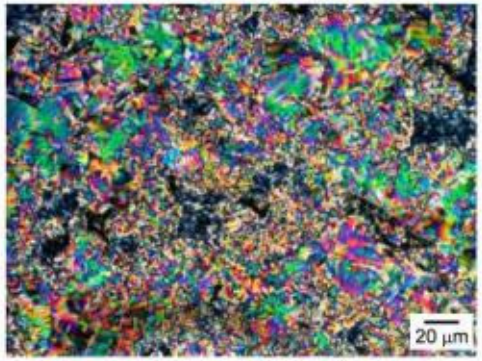

54 °C (S_X)

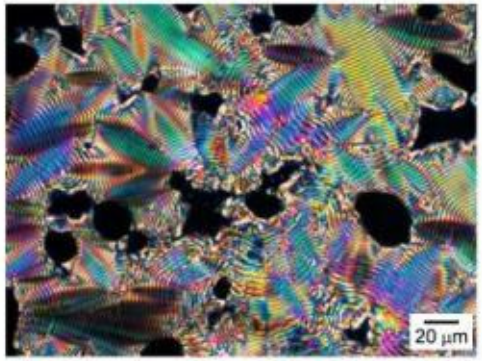

64 °C (S_C*)

Heating

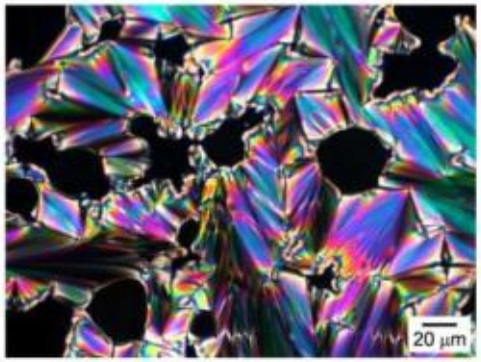

67 °C (S_A)

Continued

c

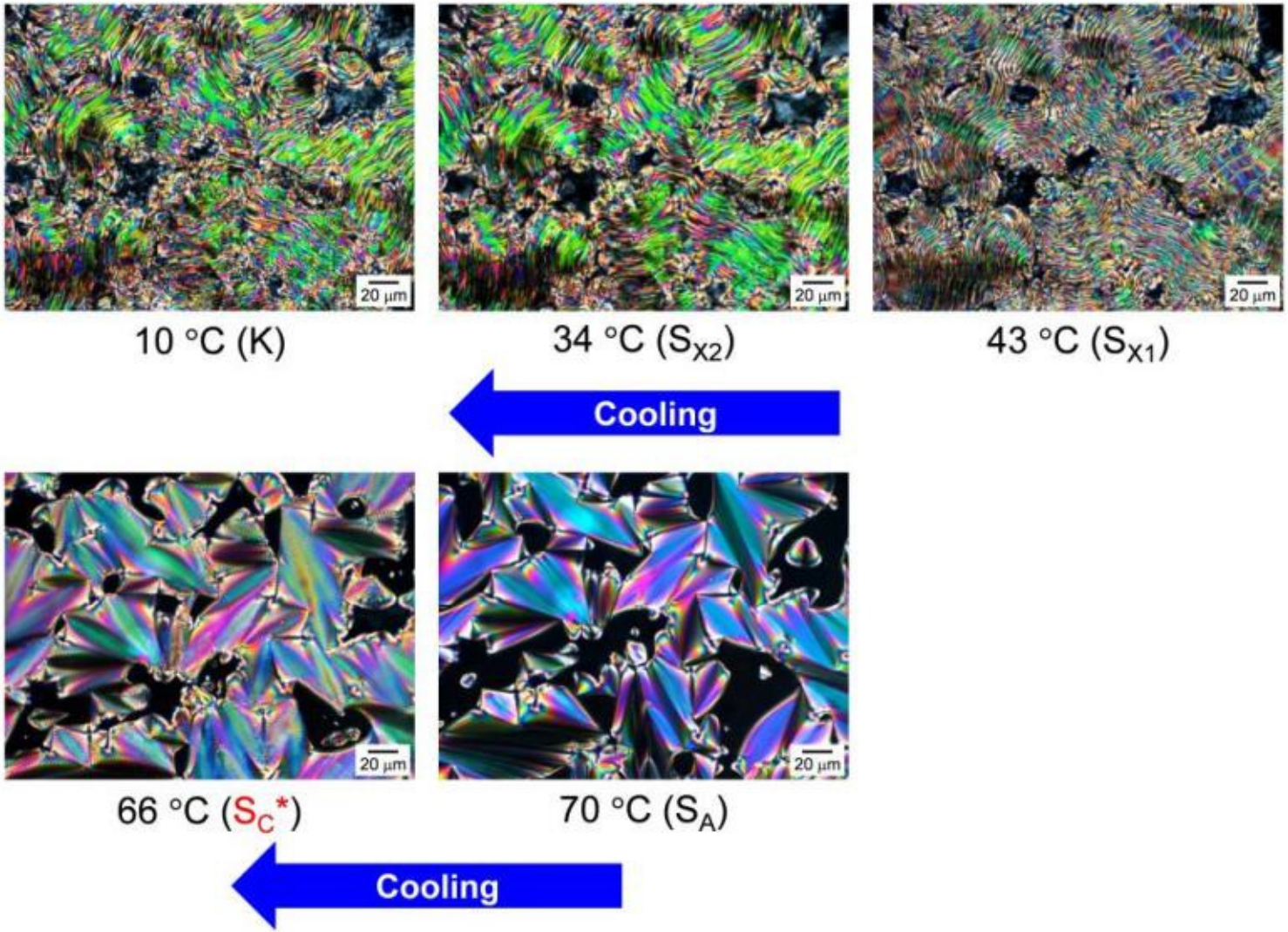
20 μm
20 μm
20 μm
10 °C (K)
34 °C (S$_{X2}$)
43 °C (S$_{X1}$)
Cooling
20 μm
20 μm
66 °C (S$_C$*)
70 °C (S$_A$)
Cooling

Figure 5. DSC thermographs and POM photographs of the host S_C-LC, **PhB1** with 1 mol% of **D-6,6'**. The DSC thermographs (a) **PhB1** with 1 mol% of **D-6,6'** were obtained with heating and cooling rates of 2 °C/min. The POM photographs of **PhB1** with 1 mol% of **D-6,6'** were taken during the heating (b) and cooling (c) processes.

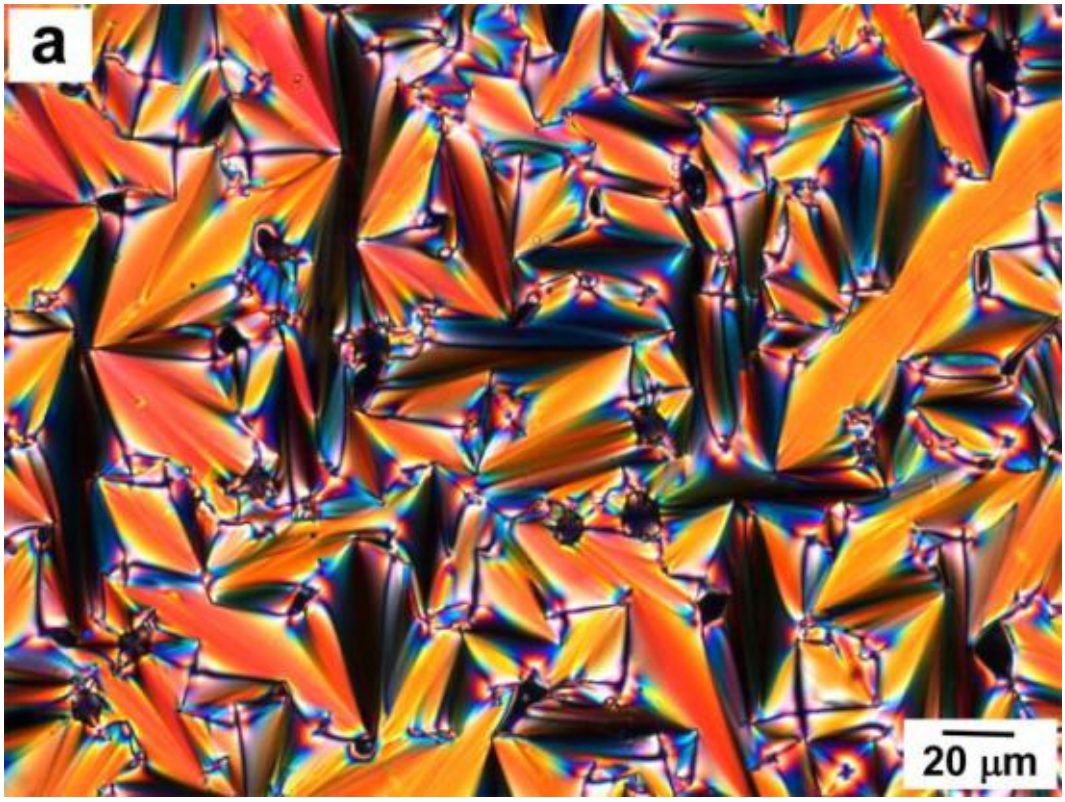

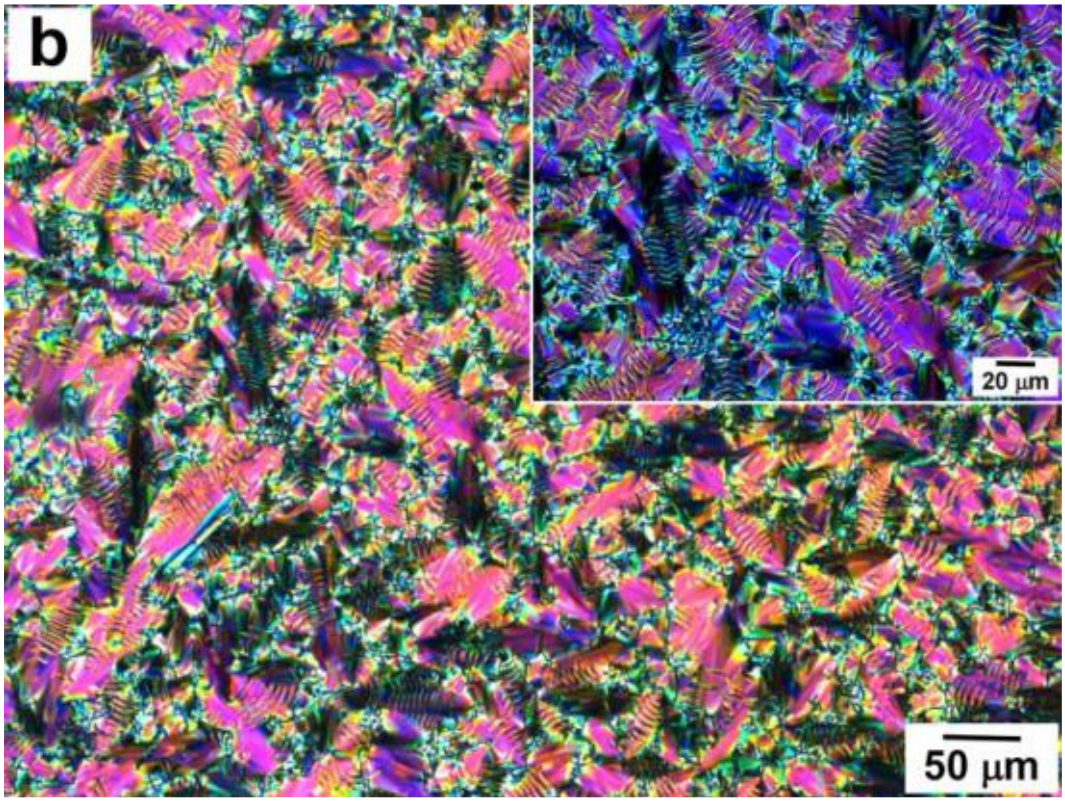

Continued

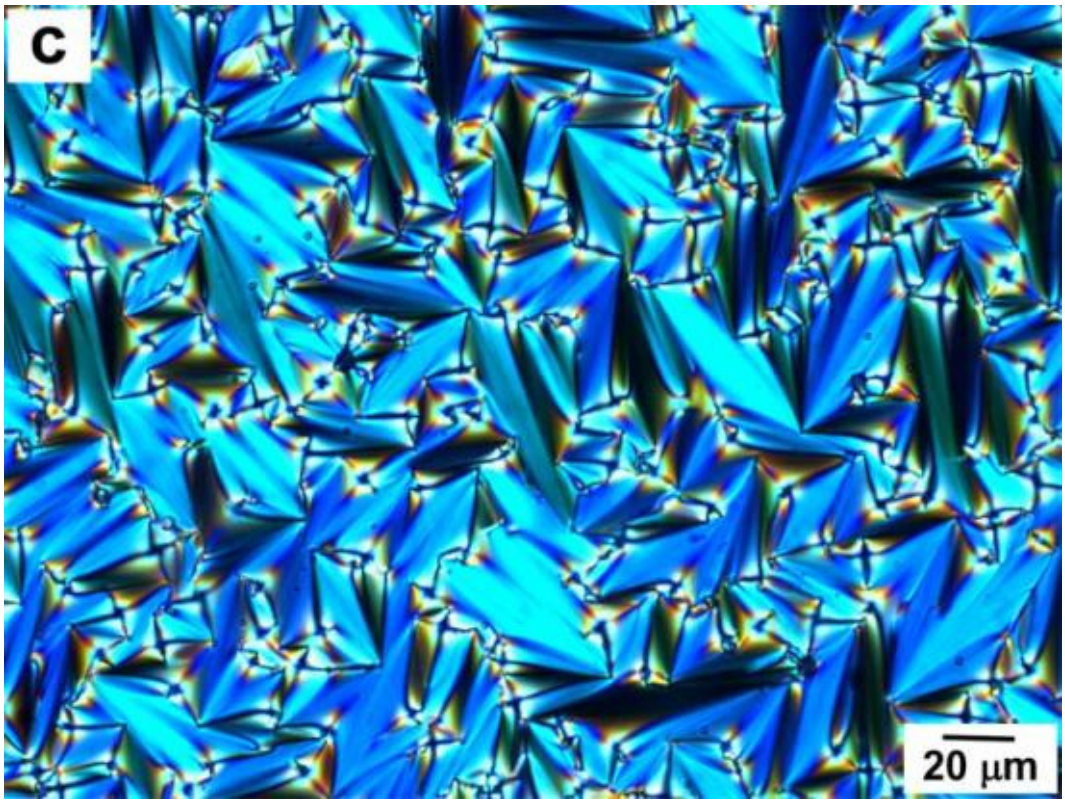

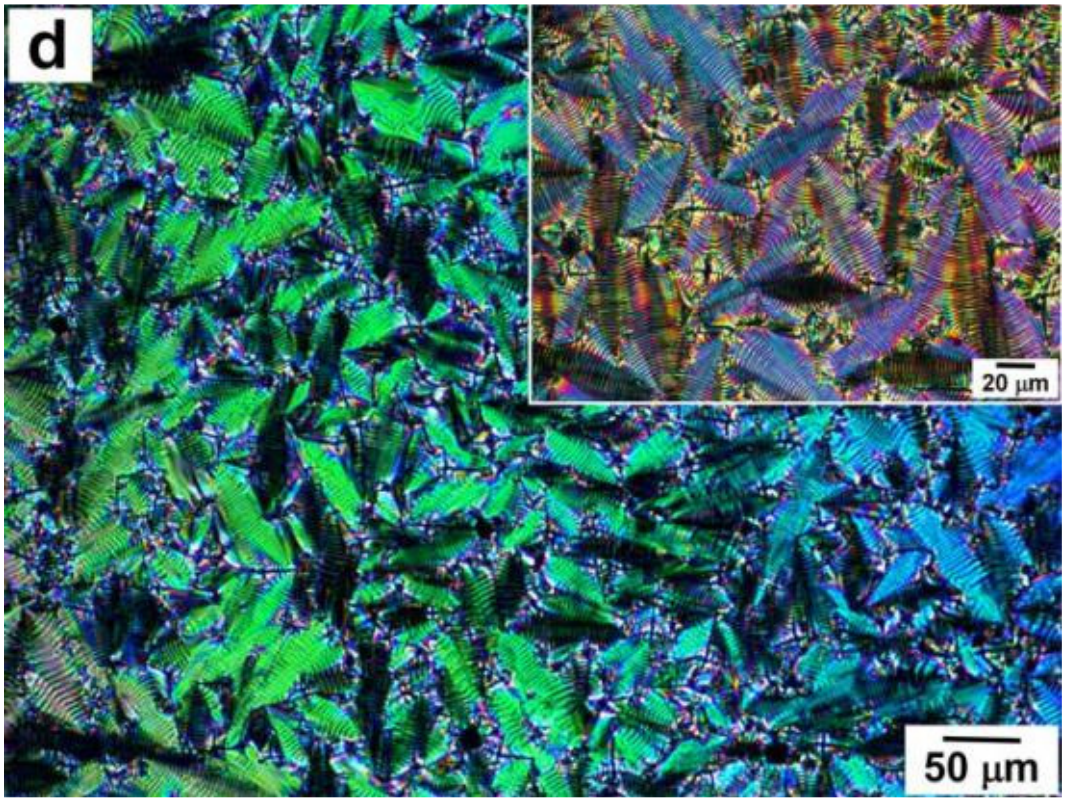

Figure 6. POM photographs of (a, c) S_A and (b, d) S_C* phases induced by the addition of 1 mol% of (a) **D-1**, (b) **D-3,3'**, (c) **D-4,4'** and (d) **D-6,6'** into the host S_C-LCs of **PhB2**.

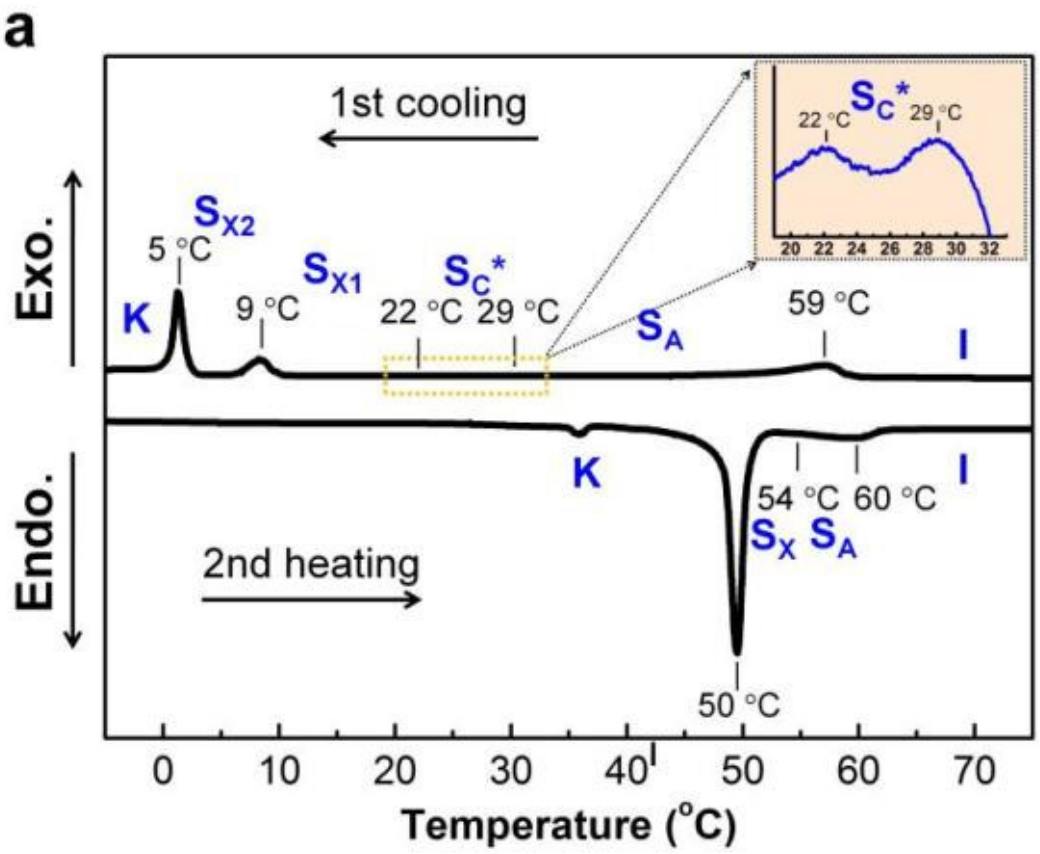

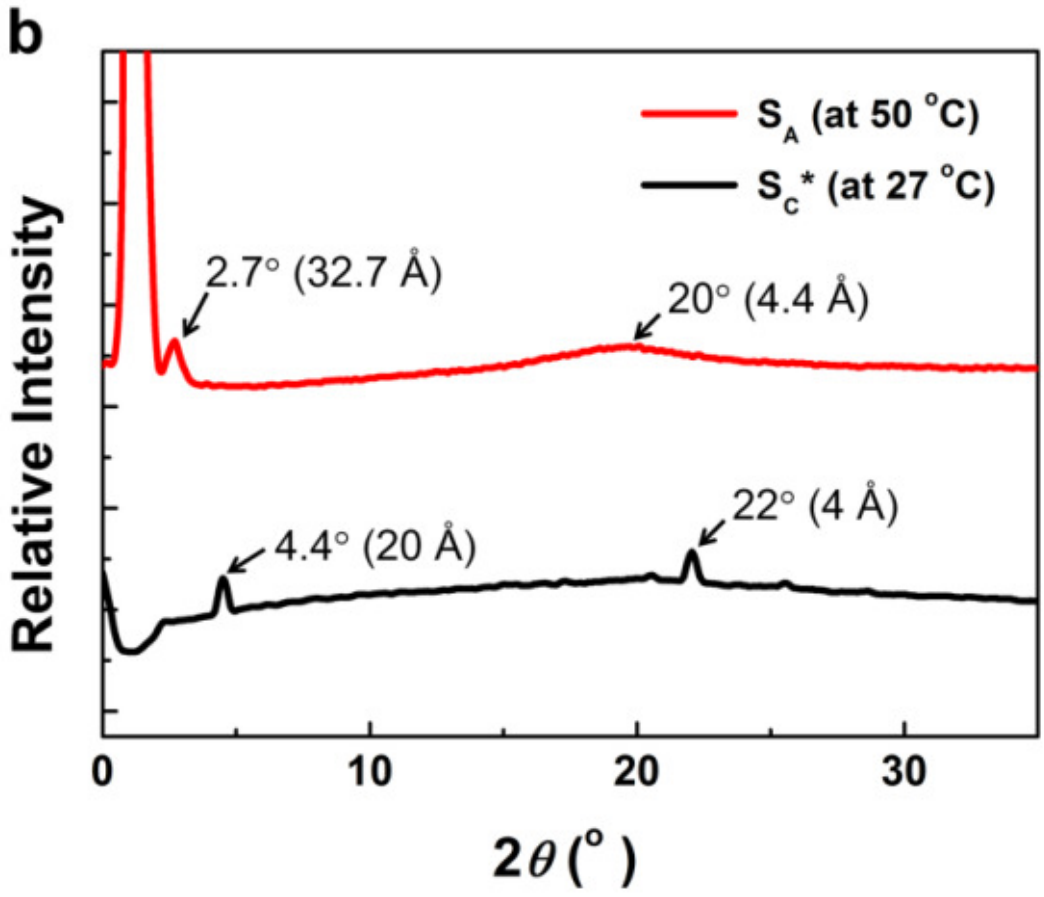

Continued

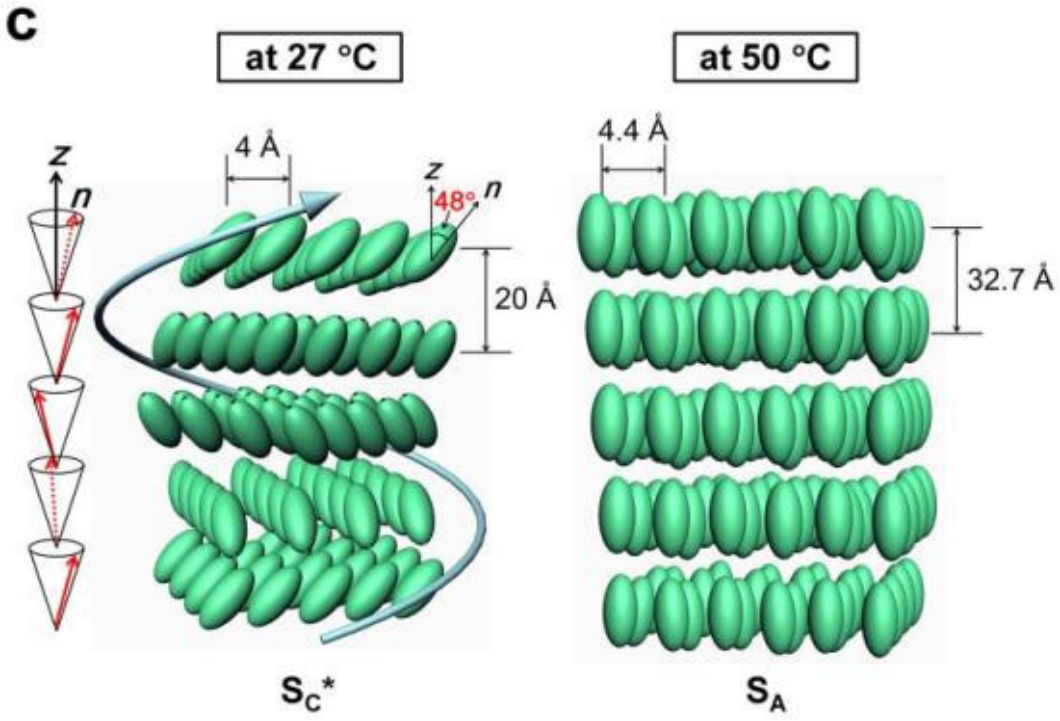

Figure 7. (a) DSC thermograph and (b) XRD profiles of **PhB2** with 1 mol% of **D-6,6'**. XRD diffractions were measured during the cooling process. (c) Schematic illustration of the molecular arrangements in the S_C* and S_A phases.

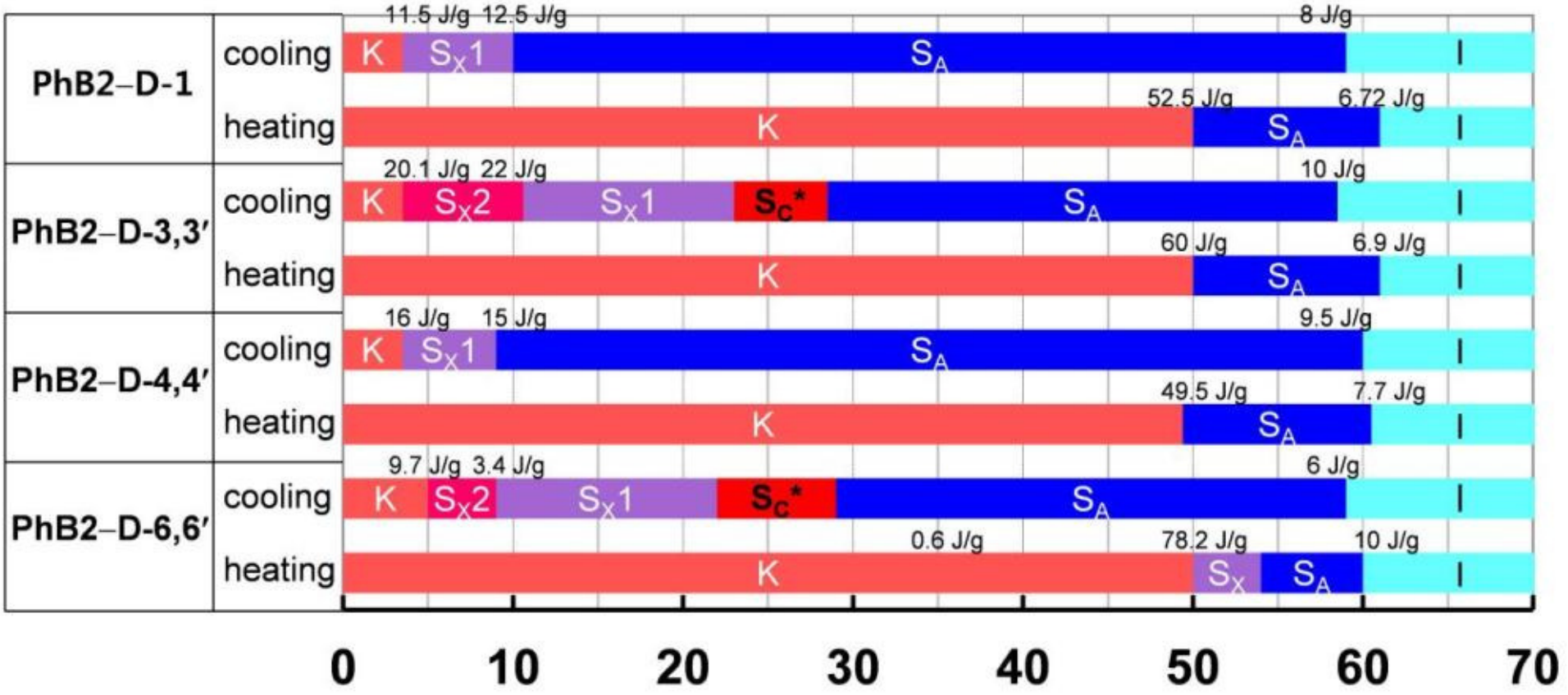

Figure 8. The phase transition temperatures (°C) and transition enthalpies [ΔH (J/g)] (measured on cooling and heating rate of 2 °C/min) of **PhB2–D-1**, **PhB2–D-3,3′**, **PhB2–D-4,4′** and **PhB2–D-6,6′**.

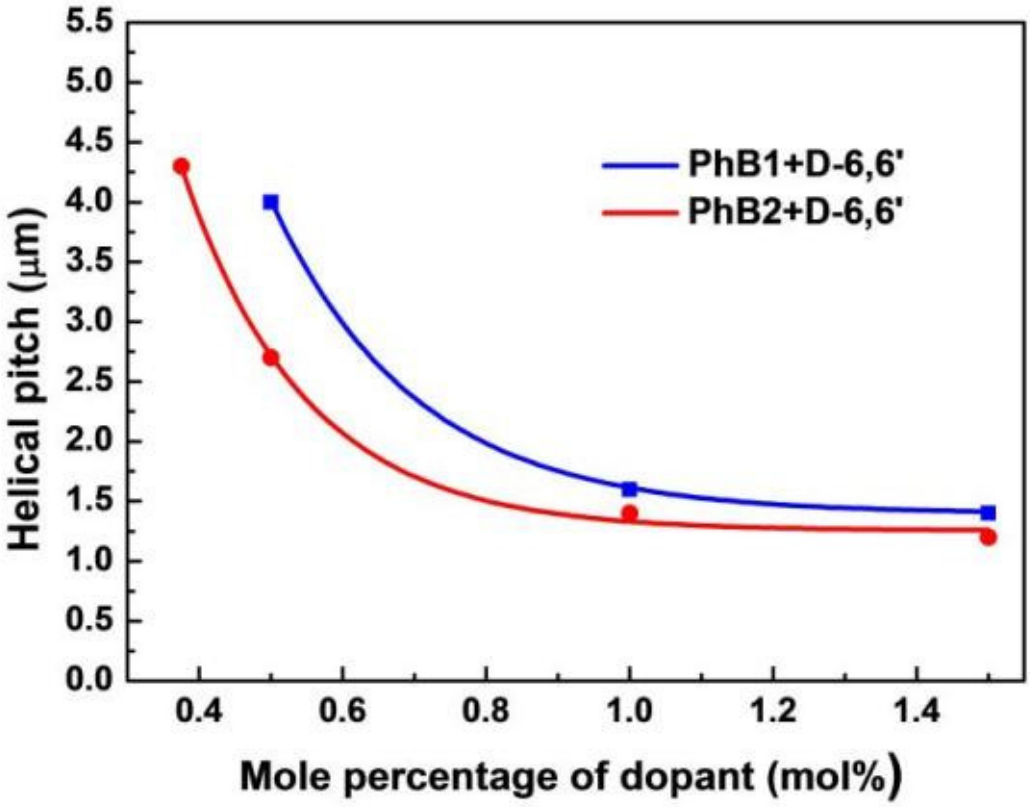

Figure 9. Changes in the helical pitch of S_C* as a function of the mole percentage of the chiral dopant **D-6,6'** added into the host LCs, **PhB1** and **PhB2**.

Table 2. Helical pitches of S_C* phases induced between host LCs and chiral dopants.

Host LC	Chiral dopant		Helical pitch[a] (μm)
	type	concentration (mol%)	
PhB1	**D-3,3'**	1.0	4.4
	D-6,6'	0.5	4.0
		1.0	1.6
		1.5	1.4
PhB2	**D-3,3'**	1.0	3.7
	D-6,6'	0.375	4.3
		0.5	2.7
		1.0	1.4
		1.5	1.2

[a] : measured at 60 °C in PhB1, measured at 27 °C in PhB2.

Graphical and textual abstract for the Table of contents entry.

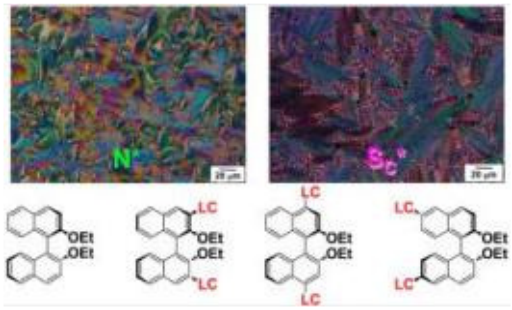

POM images of N* and S_C* phases induced by additions of atropisomeric chiral binaphthyl derivatives into N- and S_C-LCs, respectively. (20 words)